

Interactive comment on:

"A long-term study of aerosol-cloud interactions and their radiative effect at a mid latitude continental site using ground-based measurements"

Elisa T. Sena, Allison McComiskey, and Graham Feingold

We thank the editor and both reviewers for their careful review of the manuscript. The referee's comments were very constructive and they helped us improving the revised version of the manuscript. The reviewer's questions are addressed in bold, followed by the responses in normal font.

Response to anonymous reviewer 1

1. Page 2, Line 4: Absorbing aerosol could also modify the atmospheric temperature profile and stability, and reduce cloud amount via the semi-direct effect (e.g., Koren et al., 2008). Koren et al. (2008) just provide the cloud amount change with aerosol optical depth but didn't show absorbing aerosol could modify the atmospheric stability. Huang et al. (2009) use the Fu-Liou radiation model and CERES radiation flux to derived the heating rate of aerosol layer and directly show the changes in temperature profile.

Huang J., Q. Fu, J. Su, Q. Tang, P. Minnis, Y. Hu, Y. Yi, and Q. Zhao, 2009: Taklimakan dust aerosol radiative heating derived from CALIPSO observations using the Fu-Liou radiation model with CERES constraints, Atmos. Chem. Phys., 9, 4011-4021.

Answer: Thanks. This reference was included in the revised version of the manuscript.

We did look into aerosol extinction and single scattering albedo for a possible semi-direct effect but for the data considered aerosol amounts were simply too small to have an impact. This is now stated in the text.

2. Authors used the aerosol index instead of CCN concentration in this study. As the SGP site do equipped with the Cloud Condensation Nuclei Particle Counter, why do not use this data directly?

Answer: In this work 14-years of coincident measurements of aerosol, clouds and meteorological data were used. CCN concentration measurements were available at the SGP only from 2007 on. Furthermore, a complete scanning of CCN measurements over different supersaturation values takes about 1 hour. The use of CCN concentration would require the selection of a given supersaturation, which would considerably reduce the number of data points analysed. On the other hand, nephelometer light scattering measurements were available since 1998 at 1-minute resolution. To maximize the number of years included in the analysis, aerosol index (a quantity readily calculated from scattering measurements) was used as a proxy for CCN concentration. Shinozuka et al., 2015 propose a new methodology to estimate CCN (at a given supersaturation) using light scattering measurements. We have now used his approach in addition to A_i and the results are similar to the results previously obtained, as shown in Figures R1a-c, for a supersaturation of 0.6%. This new analysis does not result in changes to the main conclusions of this paper. The distribution of daily correlation between rCRE and CCN is centered at 0.02. Also, the scatter plot of the correlation between rCRE and CCN by the correlation of LWP and

CCN concentration shows a positive correlation of 0.42. These figures are included in the Supplementary section.

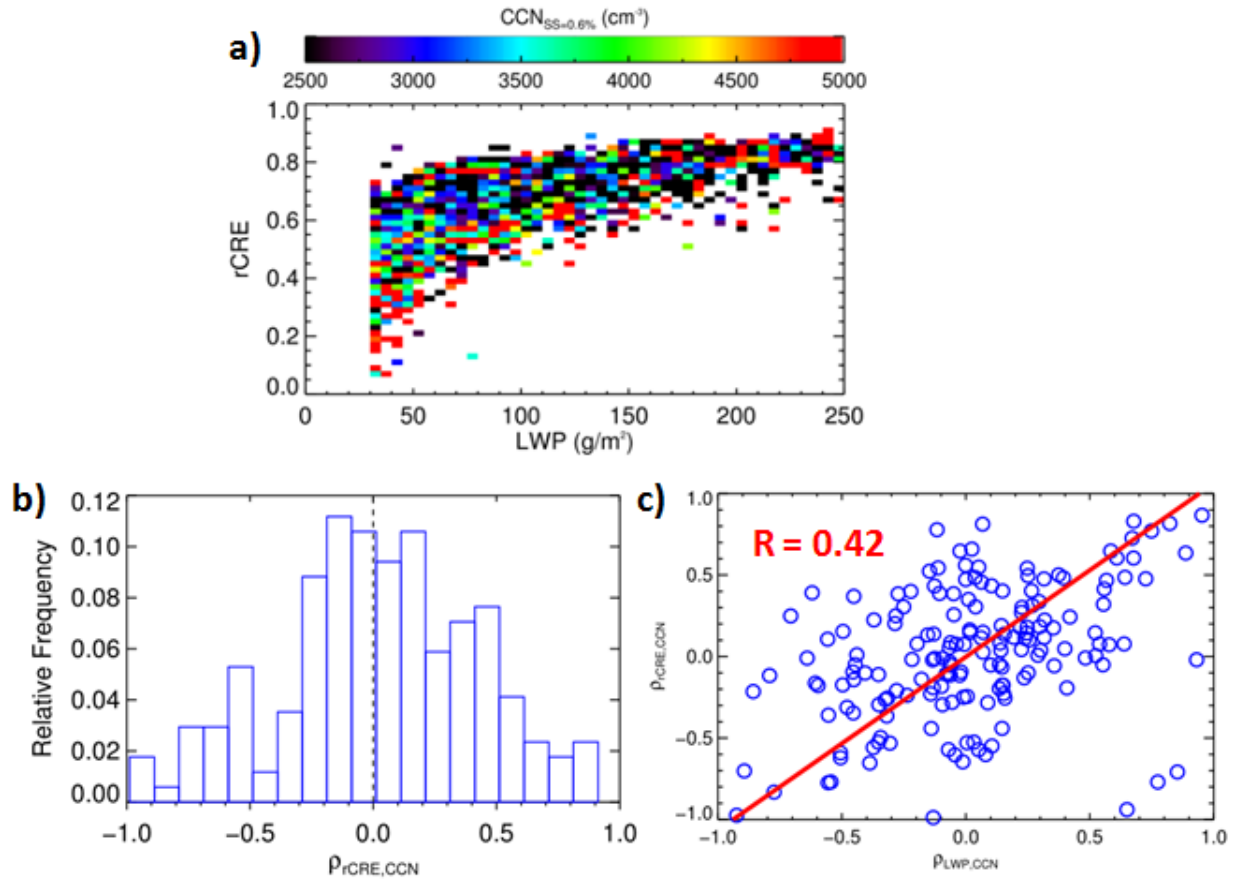


Figure R1: a) Relative cloud radiative effect (rCRE) as a function of liquid water path (LWP) colored by CCN concentration, b) daily distribution of the correlation between rCRE and CCN, and c) correlation between rCRE and CCN versus the correlation between LWP and CCN. To calculate CCN concentration, a supersaturation of 0.6% was considered.

3. Authors mentioned that all of the relevant variables were averaged to 1-minute resolution. Does this time resolution is suitable for this study?

Answer: The choice of 1-minute resolution resulted from a consideration of a number of factors such as a desire for representation of small-scale aerosol-cloud processes, large statistics, consideration of the temporal scales of variability of aerosol and cloud fields, and the recognition that averaging might be required to show clear trends. The 1-minute timescale balances these factors. A higher temporal resolution for cloud fields would have been more desirable for broken cloud fields but these are a small fraction of the current data set.

4. Koren et al. (2008, ACP) show ω (550 hPa) and RH(350 hPa) yielded the highest correlations with the satellite-derived cloud properties, these parameters will be used to represent the primary meteorological controls on the cloud system. Herein, authors examined the impact of cloud macroscopic properties (fc and τ) and meteorological variables (Di, LTS, and w'^2) on cloud radiative effect. How did authors choose those

variables?

Answer: Cloud fraction and cloud optical depth were selected because they are the two main macroscopic cloud variables related to cloud radiative properties. w^2 was used as a proxy for turbulence. Higher turbulence leads to an increase in vapor supersaturation, favoring the formation of cloud droplets. This effect could increase cloud albedo, also affecting cloud radiative forcing. D_i is a meteorological index associated with the coupling between the surface and the boundary-layer. D_i is an indicator of how well-mixed the atmosphere is below the cloud, and therefore, how well surface measurements of aerosol loading and properties represent cloud-level aerosol. LTS is another meteorological index associated with the strength of the inversion capping. This parameter is related to cloud fraction, a parameter that also influences cloud radiative forcing. A minor change was included in the text reinforcing the influence of turbulence on supersaturation.

Response to reviewer 2 - Johannes Quaas

No measurements in N_d are used in the study by Sena et al.. Rather, near-surface nephelometer measurements of the aerosol index are used as a proxy for cloud condensation nuclei concentrations (CCN) and subsequently for N_d . The results of the decomposition analysis to identify impacts of the various parameters on rCRE are presented in Fig. 3 where all three effects are convolved. More instructive still is Fig. 5 where only overcast cases are selected. At the theoretical level (Eq. 8 and 9), for a given LWP bin, rCRE can only be a (strictly monotonically increasing) function of N_d . In light of this, the results are puzzling. There is no clear relationship of rCRE at given LWP with near-surface aerosol index (Fig. 5a). There is no influence of w on rCRE (Fig. 5b). There is, however, a more systematic influence of the decoupling index and also of lower-tropospheric stability (LTS). The authors interpret that the aerosol impact is small. This is a straightforward interpretation of Figs. 5a and 6a. But how can this conclusion be true? Does this not imply the simple theoretical model in Eq. 8 and 9 is wrong? The other possible explanation is certainly that the nephelometer measurements near the surface are not a good proxy for in-cloud N_d . Perhaps one could test this by trying to relate remote sensing retrievals of N_d to the aerosol index?

Answer: The simple two-stream theoretical model from Eq. 8 is useful to provide insight into the expected behavior of rCRE with LWP and N_d . It shows that the impact of LWP on rCRE is much larger than the impact of N_d , based on the fact that cloud optical depth is proportional to $LWP^{5/6} N_d^{1/3}$; i.e., in a relative sense, cloud optical depth is 2.5 times more sensitive to LWP than it is to N_d . However, this simple model does not account for several different conditions experienced during an actual measurement, e.g., 3D radiative effects, near-cloud radiative absorption, changes in atmospheric stability, dry air entrainment and non-adiabatic processes. On the other hand, Figs. 5a and 6a are a result of 'actual' ground-based measurements of rCRE, LWP and A_i . They represent the bulk result of the interaction of all processes affecting cloud radiative properties. Eq. 8 represents a highly simplified system where 'all else' must be equal and uncertainty in the terms is not allowed.

The lack of coupling between aerosol concentrations at the surface and cloud base could also explain this result; this is addressed elsewhere in the paper and in the responses below.

Following the reviewer's suggestion, we have looked at ground-based remote sensing retrievals of N_d using column properties LWP and τ_c . A clear trend is observed when plotting rCRE vs. LWP colored by N_d (Figure R2). This clear aerosol influence is, however, a result of the fact that the N_d and rCRE data are no longer independent due to the retrieval method. We have stressed in previous work that an independent estimate of N_a and/or N_d is critical for such studies.

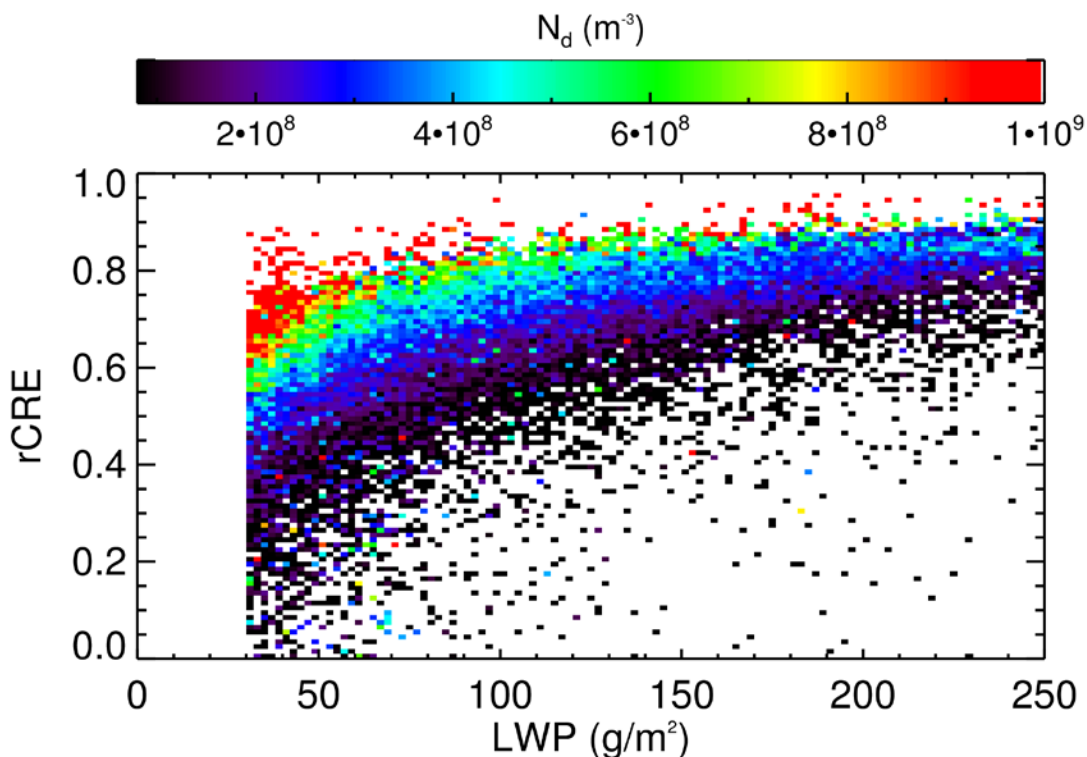


Figure R2: rCRE as a function of LWP colored by N_d .

On the other hand, A_i (or other CCN proxies, such as Shinozuka et al., 2015) are independent measurements of the aerosol that might affect cloud properties. They do not rely on the retrievals of macroscopic cloud properties themselves, as do N_d retrievals. The decoupling index is an indicator of how well-mixed the atmosphere is, and therefore, how efficiently aerosol particles are transported to higher levels of the atmosphere. Therefore, low D_i values could indicate conditions under which surface-based aerosol measurements represent cloud-level aerosol. To overcome this issue, in the manuscript the daily correlation between rCRE and A_i was calculated for low and high D_i values (Fig. S3). No differences were observed (both distributions were centered around 0). These results are supported by the findings of Delle Monache, 2004, referenced in the paper and discussed later in this response. In addition, Shinozuka's (2015) proxy was used to calculate CCN (see Figs. S1a-c in response to referee 1). To consider only well-coupled conditions, only low D_i values were selected. Again, the conclusion didn't change. Under these conditions, the distribution of daily correlation between rCRE and CCN is centered at -0.04. The scatter plot of the correlation between rCRE and CCN by the correlation of LWP and CCN concentration shows a high positive correlation, of 0.57 (Figures R3a-b).

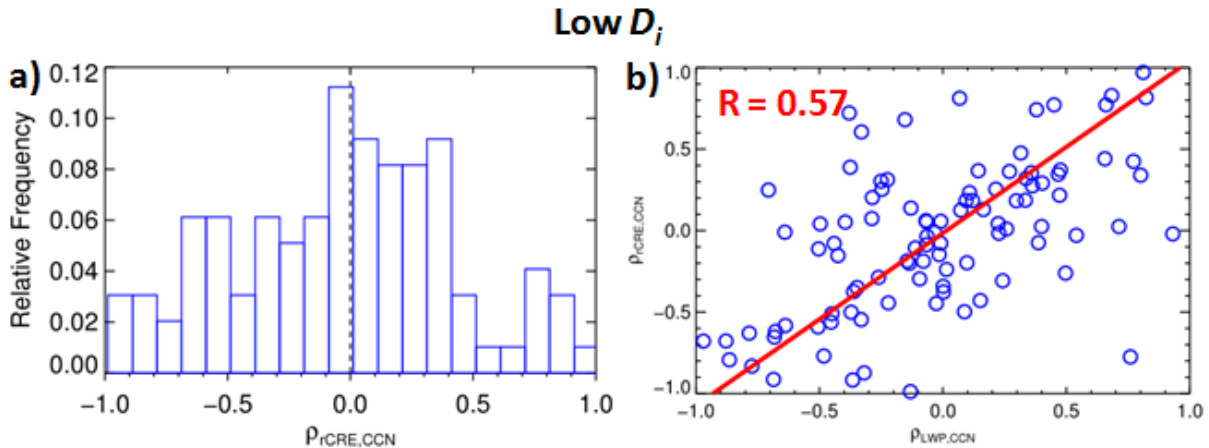


Figure R3: a) Daily distribution of the correlation between rCRE and CCN, and b) correlation between rCRE and CCN versus the correlation between LWP and CCN, for well-coupled conditions ($D_i < 0.25$). To calculate CCN concentration, a supersaturation of 0.6% was considered.

A very interesting question is further, why is there the impact of decoupling index (Fig. 5c) and LTS (Fig. 5d), but not of w ? My own experience would point to spurious variability in LWP and cloud fraction that the binning into bins of 5 g m^{-2} and the constraint of the retrieved cloud fraction at 100% is not able to completely inhibit. Given that despite the length of the data record not overly much data is available due to the conditioned sampling, an option would be to use coarser bins and see whether the effects are larger.

Answer: Actually there is a weak trend of rCRE increasing with decreasing w^2 . This weak trend is associated with the types of clouds associated with each w^2 range. Usually, broken-cumuli are associated with higher convection, therefore higher w^2 , and lower cloud fraction. On the other hand, stratiform-like clouds are associated with lower convection (lower w^2), and higher cloud fraction. Lower (higher) cloud fraction leads to lower (higher) rCRE.

To understand the impact of spurious data, we have tried several LWP binning schemes, as suggested. We have found that changing the binning does not change the general behavior of the curve. Figure R4 shows an example of a different binning scheme, using 20 g/m^2 for the LWP bin.

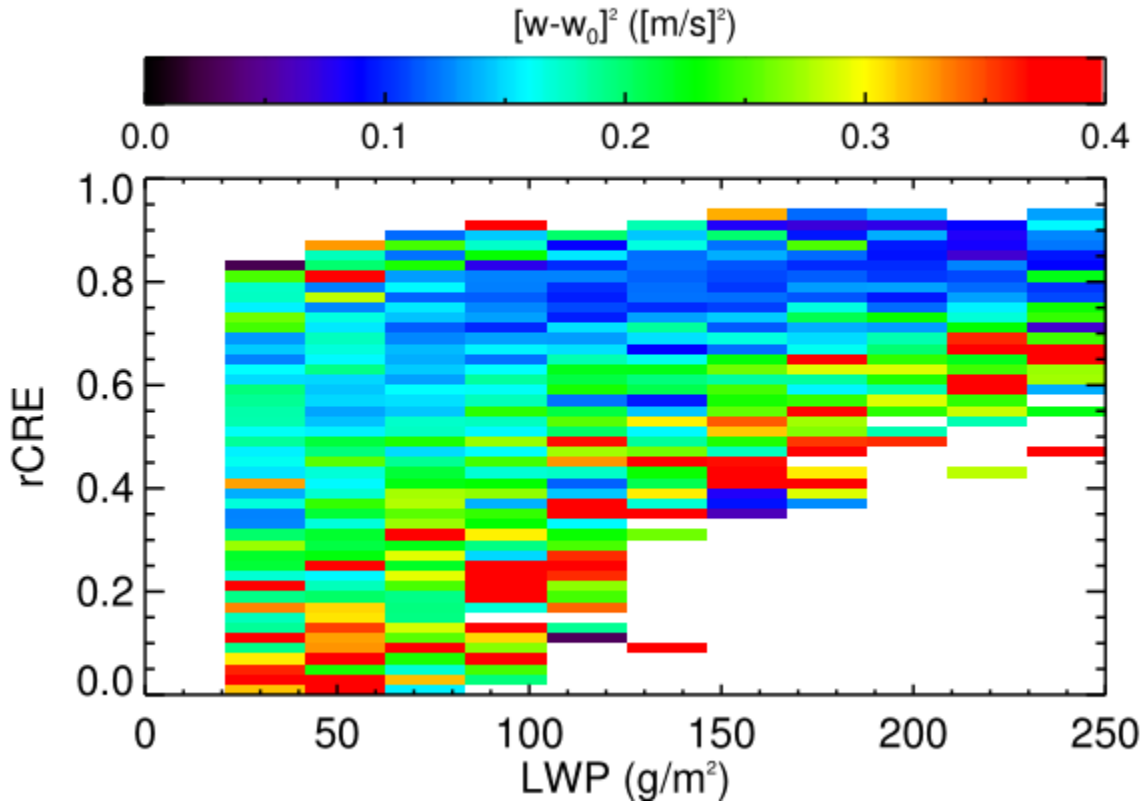


Figure R4: rCRE by LWP colored by w^2 (LWP bin: 20 g/m^2).

Else it is possible that the retrievals of either rCRE or LWP somehow depend on decoupling index or on LTS, but I am not enough of an expert on the retrievals to say whether this is possible. Another possibility is that the diurnal cycle in the decoupling index (Fig. 12) impacts rCRE more strongly than one might anticipate via the not-eliminated impact of the solar zenith angle (Eq. 8).

It would be very useful if the authors could discuss these questions in order to understand to which extent the “negative” or “null” result of no influence of aerosols on rCRE is a robust finding.

Answer: rCRE does depend on D_i or LTS via the dependence of primary factors such as f_c and LWP on D_i and LTS but we see no reason why the *retrievals* of rCRE or LWP would be. The first algorithms used for LWP retrievals (Liljegren et al., 2001) could present some biases regarding D_i , as they used a statistical site-dependent approach, based on monthly coefficients dependent on near-surface temperature estimates. However, in this work, the MWR retrieval (MWRRET) value-added-product algorithm was used. This algorithm has been significantly improved and relies on physical retrievals of the temperature profile. Therefore, we don't see any reason for LWP retrievals to depend on D_i .

You are right: there is a non-eliminated relationship between rCRE and solar zenith angle on the two-stream theoretical model presented in Section 2. rCRE varies slowly with θ_0 for lower θ_0 values, but shows a strong dependence on θ_0 for higher angles. Figure 3 provides useful information, but includes another degree of variability in the data (θ_0), that prevents us from immediately attributing changes on rCRE to the other variables. Therefore, this intrinsic

dependence of rCRE on θ_0 does not allow us to isolate the effects due solely to other properties on rCRE from the effects caused by solar illumination. To reduce this influence, another figure was included showing the dependence of rCRE on LWP colored by the same variables of Figure 3, but considering only cases obtained when $\cos(\theta_0) \geq 0.6$. This limit was selected such as to maximize the amount of data analyzed and at the same time, minimize the effects of solar illumination on rCRE. As D_i , w'^2 and f_c are highly correlated and have a very marked diurnal cycle (and therefore an association with solar zenith angle) we cannot separate the impacts of D_i (and f_c) and solar zenith angle on rCRE on Figure 3. The new analysis, obtained after restricting the solar illumination angle, shows that the general trends of rCRE do not change for aerosol and τ_c , when θ_0 is limited. However, for D_i , f_c , w'^2 and LTS the rCRE trends at a fixed LWP value previously observed in these figures are reduced. One of the explanations for this behavior is that, as these variables have a marked diurnal cycle; limiting θ_0 significantly reduces their variability. For example, higher D_i values are usually observed during early-morning and late afternoon. Therefore when only low θ_0 values are considered, these higher D_i observations will not appear as frequently in the data set. On the other hand, as higher LWP values are associated with higher f_c , higher D_i and lower w'^2 values, high rCRE values will likely be observed when these macroscopic properties and thermodynamic conditions are met. These points are now discussed in the manuscript. As this comment generated so many interesting and fruitful discussions we have decided to include both, the θ_0 -restricted and non-restricted figures in the manuscript (Figures 3 and 5 in the new version). For the other analysis (A_c vs. LWP, daily distributions of $\rho_{\text{rCRE,LWP}}$ and $\rho_{\text{rCRE,Ai}}$, correlation between $\rho_{\text{rCRE,Ai}}$ and $\rho_{\text{Ai,LWP}}$) only the more restrictive condition for θ_0 was used. It is worth mentioning that when we limit θ_0 , the daily correlations between rCRE and LWP increased significantly, and 98% of the cases show positive $\rho_{\text{rCRE,LWP}}$. Also, in the last figure the correlation between $\rho_{\text{rCRE,Ai}}$ and $\rho_{\text{Ai,LWP}}$ increases to 0.71. These results indicate that variations in θ_0 might have been obscuring the relationships. The figure of the distributions of $\rho_{\text{rCRE,Ai}}$ for low and high D_i conditions (Fig. 7 in the previous version of the manuscript) was removed, because when θ_0 is restricted only low D_i remain in the database.

The authors also conclude that microphysical metrics in general are misleading. This conclusion mainly stems from the results in Table 2. While there is probably consensus that retrievals of cloud microphysical quantities are error-prone, such a broad conclusion should be corroborated better. If the authors decide this is a focus of the paper, then they should include a much more detailed discussion and ideally evaluation of the three different retrieval algorithms for the effective radius and explain why all three are (equally?) valid. In this regard, it should be noted that retrievals of microphysical quantities from the surface in general are more difficult than from the top of the atmosphere (Brueckner et al., J. Geophys. Res., 2014 doi: 10.1002/2014JD021775)

Answer: Our intent is to focus the results of this paper on the influence of LWP and cloud macrophysical properties on rCRE in a statistical sense. Microphysical metrics, when used carefully, can likely provide a quantification of aerosol influences on cloud microphysical properties, and at the very least a test of self-consistency. However, transferring that value to a statistically representative rCRE is not as straightforward as the literature has assumed in the past. This issue is not the focus of the current paper but has been dealt with in some depth in earlier works (McComiskey et al. 2009; McComiskey and Feingold 2012).

We are quite interested in the results of Table 2 and plan to look further into these difference and better understand the retrieval uncertainties in general. Regarding the Brueckner reference we disagree that space based retrievals are in general easier than surface based retrievals, unless of course the surface microphysical retrievals are based on transmission, which then generates ambiguous results (Sebastian Schmidt and colleagues; Brueckner). None of our microphysical retrievals uses transmission as in those works so we feel it would be a distraction to engage in discussion of this topic. Given our focus on the current work, and our earlier efforts on ACI metrics, we do not feel that an in depth examination of retrieval uncertainties would fit within the current work.

Besides these two main comments, I have a few specific comments listed below.

Specific comments

Title: Why not name the ARM SGP site?

Answer: The title was modified and now mentions "the Southern Great Plains" explicitly.

Abstract p1 118: I think that in the abstract “weak” needs quantification. One would expect the aerosol to be second order anyway.

Answer: The following sentence was added to the abstract: "On a daily basis, aerosol shows no correlation with cloud radiative properties ($R = -0.01 \pm 0.03$) whereas liquid water path shows a positive correlation ($R = 0.56 \pm 0.02$)".

P1 129: Most publications currently would suggest additional effects due to microphysical adjustments, not so much a compensation (e.g. Lohmann and Feichter, Atmos. Chem. Phys. 2006)

Answer: In the original sentence we talk about both: "mutually compensating effects and adjustments". We don't think a change is necessary.

p2 16: I think we should in general aim to be more specific about what we mean by “meteorology”.

Answer: In order to be more specific, the sentence was modified to: "The influence of meteorological drivers and thermodynamic conditions (e.g., atmospheric stability and humidity) on aerosol-cloud interaction assessments is increasingly being brought into focus".

P2 119: It would be useful to discuss Bender et al. (J Climate 2015 doi 10.1175/JCLI-D-15-0095.1)

Answer: Thanks for raising this. The main point of this paper is that for marine stratocumulus regimes, at a fixed cloud fraction, total albedo is controlled by temporal rather than spatial variability. This is a bit off topic and despite our efforts, we couldn't find a place to insert this idea without breaking the flow of the paper.

P2 127: It would be appropriate to cite Li et al. (Nature Geosci 2011, doi 10.1038/NGEO1313) here.

Answer: We have modified our text to say: "The availability of such a large and comprehensive dataset provides an excellent opportunity to pursue a long-term study of the effects of aerosol and meteorology on the cloud radiative effect."

Li et al. addressed aerosol effects on precipitation. We have concerns about the way aerosol (CN rather than CCN), thermodynamics and macroscopic variables were taken into account in Li et al., 2011's paper and therefore chose not to cite it in the manuscript.

P2 I29: Again it would be good to specify what is meant by “meteorology”

Answer: The sentence was modified to "14-years of ground-based measurements at the SGP were analyzed to investigate the effects of aerosol and meteorological drivers (such as capping inversion strength, surface-boundary layer coupling and turbulence) on clouds".

p3 I13: abbreviate second as “s”

Answer: Done.

p3 I20: overcast at which scale (1 min \approx 600 m for 10 m/s wind speed?)

Answer: In this context, overcast conditions are considered on the scale of hundreds of meters. The average wind speed is around 6 m/s (1 min \sim 360 m). This information is now included in the revised manuscript.

P2 I8: “s” instead of “second”

Answer: Done.

p4 I31: this is only true on climatological (monthly-mean) time scales (e.g. Nam and Quaas, Geophys. Res. Lett., doi:10.1002/grl.50945)

Answer: Some studies point out the relationship between LTS and f_c on climatological (monthly-mean) time scales. However, Chen et al., Nature Geosc., 2014 point out the importance of LTS on cloud liquid water responses on a much shorter timeframe. In their work, instantaneous ECMWF reanalysis data are interpolated for each CloudSat cloud radar profile. This reference is now included in the newest version of the manuscript.

p5 I2, I4: minute \rightarrow min

Answer: Done.

p5 I12: the stricter criterion was second in the earlier sentence

Answer: Thanks for noticing it. The order of the sentence has been inverted in the new version of the manuscript.

p5 I18: This is an interesting result. Is the conclusion that clouds are independent of the turbulence and other boundary-layer properties, at least with regard to the LWP?

Answer: We cannot affirm that clouds (or specifically LWP) are independent of these properties based only on the analysis of these histograms. Figure 1 only shows that the distributions of turbulence, D_i , LTS and A_i do not depend significantly on the higher and lower end of the LWP distribution (30-50 g/m^2 and 150 - 250 g/m^2). However, to address the influence of these boundary-layer properties on clouds would require a much more rigorous analysis that delves into the full meteorological context of these data.

P5 I24: It would be useful to also list the other numbers: what is the fraction of data-points

with $f=1$, what with $f > 0.99$?

Answer: The fraction of data points with $f_c=1$ (or $f_c > 0.99$) is 79%, for LWP between 50 and 150 g/m^2 and 75% for LWP between 30 and 250 g/m^2 . This information is now included in the revised manuscript.

P5 127: To which extent are these two quantities independent at all? Is not actually one derived from the other one (Table 1)?

Answer: These quantities are not derived from each other, but they are closely related. According to Xie and Liu, 2013 the relation shown in equation (4) holds if we consider surface albedo = 0 and neglect cloud absorption of radiation. As usually surface albedo $\ll 1$ and cloud absorption is small, equation (4) is a good approximation for rCRE.

p8 111: Why this choice? Why not choosing bins such that each contains the same amount of data?

Answer: The statistical distribution of LWP is asymmetrical and would typically require geometrically increasing bin width. However the lack of noise at the higher end of the LWP distribution suggests that there is no need to change to a geometrical bin structure. The binning choice used in the original manuscript makes the plot fairly symmetrical, using easy-to-read intervals (0.02 and 5 g/m^2 , for rCRE and LWP, respectively). rCRE varies from 0 to 1, leading to 50 bin intervals. LWP varies from 0 to 250 g/m^2 (even though, only measurements with LWP $> 30 \text{ g/m}^2$ were considered), also leading to 50 bin intervals. As shown above, we see no significant change in results for a different LWP bin width.

P8 117: But Fig. 3e still shows considerable f changes that dominate rCRE variability at low LWP.

Answer: True. This is associated with the small amount of clouds with lower f_c that bring down the average f_c as explained in the text. The following sentence is now included in the manuscript: " Figure 3e shows considerable f_c changes that dominate rCRE variability at low LWP." We believe the explanation was already in the text: "Some rCRE differences could be related to the relatively small number of broken cloud events that: i) reduce rCRE due to the smaller f_c associated with this cloud type; and, ii) introduce the possibility of three-dimensional radiative effects (e.g., Wen et al. 2007), and therefore deviations from the simple two-stream model approximations that form the basis of the rCRE analysis".

P9 11: Discussion perhaps on negative relation between τ and rCRE for lower LWP?

Answer: We don't see a negative relation between rCRE and τ_c at low LWP.

P9 112: can one tease out the result more clearly e.g. by averaging over the LWP bins?

Answer: Figure R5 shows w^2 averaged over LWP bins. For LWP $< 100 \text{ g/m}^2$, w^2 decreases with increasing LWP. This is mostly driven by the larger number of broken cumuli that have lower f_c , lower LWP and higher w^2 . As LWP increases, the number of broken cumuli in each LWP bin decreases, f_c increases and w^2 decreases. As LWP reaches higher values, almost no broken-cumuli are observed, the number of observations decreases (Fig. 1a) and therefore w^2 saturates and becomes noisier.

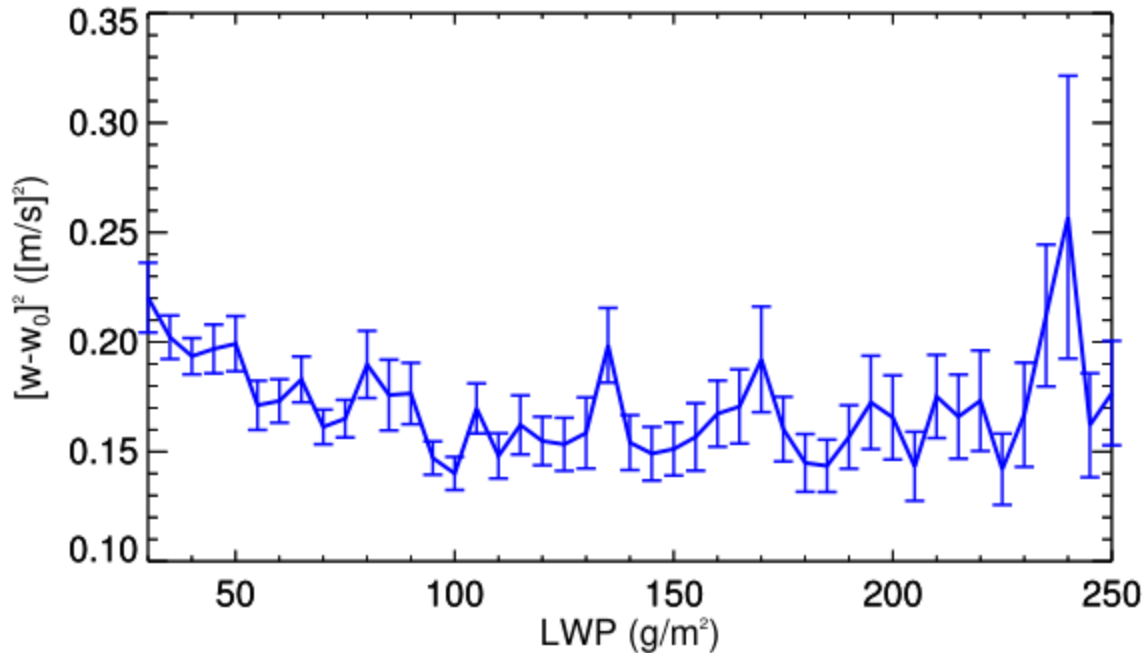


Figure R5: w'^2 averaged according to LWP bins. The error bars represent the standard deviation of the mean value of w'^2 .

P9 I12: “this result suggests” → “this result confirms” (as this important point was discussed and explained earlier)

Answer: Done.

p9 I17: again, only on monthly timescales

Answer: As previously pointed out, the impact of LTS on cloud liquid water responses was verified at a much shorter timeframe (Chen et al., Nature Geosc., 2014).

p9 I25: as before “These results indicate” → “These results confirm”

Answer: Done.

p9 I31: good idea! How many points remain? Maybe show a joint histogram?

Answer: Figure R6 shows the joint histogram of cloud albedo and LWP for overcast conditions ($f_c = 1$). This figure will be included in the Supplementary section.

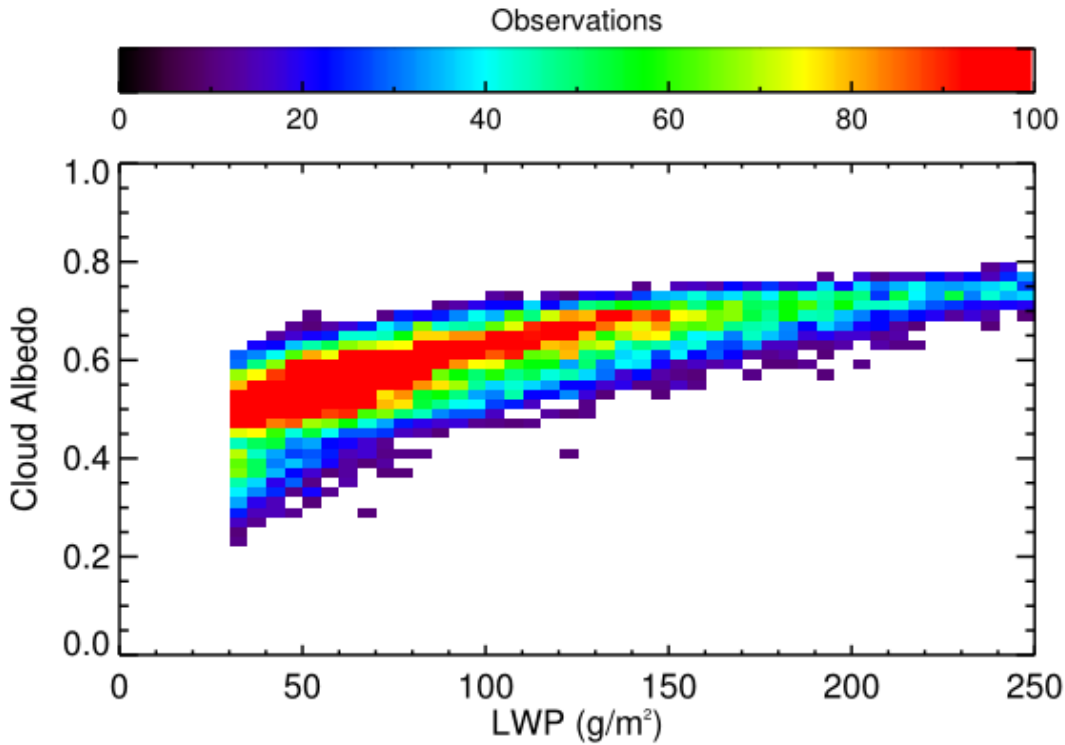


Figure R6: Joint histogram of cloud albedo and LWP for fully overcast conditions ($f_c = 1$).

P9 I32: interesting result. What could be the interpretation?

Answer: This figure was removed in the new version of the manuscript. As previously pointed out by the referee and discussed here, rCRE increases with θ_0 . As high D_i values are observed at times of the day when θ_0 is high, due to its diurnal cycle, it is hard to attribute this increase in rCRE solely to an increase in D_i . This increase in rCRE could be due to changes in θ_0 . The same analysis was performed using only data obtained when $\cos(\theta_0) \geq 0.6$. This new analysis does not show significant changes of A_c with any of the analyzed variables. This discussion was modified in the new version of the manuscript.

P10 I11: for LWP bins? Or all data?

Answer: For this analysis all data with LWP between 50 and 150 g m^{-2} were used. Cases that had less than 25 observations per day were excluded from the analysis.

P10 I18: How can a conclusion about cloud-level aerosol conditions be drawn from these results?

Answer: Under well-mixed (coupled) conditions surface-based measurements of aerosol would represent well cloud-level aerosol. In the old version of the manuscript Fig. 7 showed no significant difference between well-coupled and poorly-coupled conditions. Delle Monache et al., 2004 show that, at SGP, extensive and intensive aerosol properties measured at the surface and within the atmospheric boundary layer are well-correlated. Therefore we contend that at SGP surface-based measurements of aerosol properties are representative of the air within the atmospheric boundary-layer. In the new version of the manuscript this Figure and this excluded were removed, since only well-coupled conditions (low D_i) remained when solar zenith angle

was limited. However, as we consider Delle Monache's results a crucial point for the present analysis, the discussion on this paper was significantly extended in Section 2 of the new version of the manuscript.

P11 I12: RH measured where?

Answer: RH was measured at the surface. This information was included in the new version of the manuscript.

P11 I23: to have a physically more consistent equation, use the density of liquid water in the denominator (and then all quantities in SI units, or whatever consistent units)

Answer: The equation was modified according to the suggestion above.

p11 I26: typical for this type of scale and measurements, one should probably add and cite McComiskey and Feingold (2012)

Answer: This reference is now added to the revised manuscript.

p14 I6: An obvious way to overcome the problem of variable LWP is to use droplet number concentration retrievals instead.

Answer: As previously discussed, ground-based remote sensing retrievals of N_d are done using LWP and COD. Therefore, LWP, COD and N_d retrievals are not independent.

P15 I1: This conclusion seems only to stem from the examination of the three different effective radius retrievals. If this is intended as a main conclusion, more information about the retrievals is necessary, including some discussion on how reliable each one of these is.

Answer: Even though this is an important finding, this is not the focus of this paper. Entering details and understanding all the intricacies involved in these retrievals and their uncertainties would require the development of a complete new work. Our experience with ACI metrics at SGP and our comparisons with independent work (Kim et al. JGR 2009; doi:10.1029/2003JD003721) has left us with significant concerns about the robustness of ACI retrievals. So while we only show a small sample of cases here, we are confident that the problem is endemic. When stating generally that microphysical metrics are not always reliable, we also consider the uncertainty presented in the literature concerning cloud microphysical properties from active remote sensing techniques.

p15 I4: “meteorological conditions” should better be explained. What actually is meant here is co-variability of the aerosol with cloud macroscopic quantities (LWP in particular), I believe.

Answer: True. The sentence has been modified accordingly in the manuscript.

P15 I7: “meteorological drivers”, or rather liquid water path and cloud fraction?

Answer: You are right. We didn't mention the macroscopic cloud properties before. The sentence was modified to "relative effects of aerosols, macroscopic cloud properties and meteorological drivers". We decided to maintain the expression "meteorological drivers", as we also analyzed variables related to turbulence, capping inversion and atmosphere-surface coupling.

p16 References Abbreviate journal names appropriately (many instances) Barnard et al. (2008): correct journal name

Answer: Done.

p26 Figure 3: add a joint histogram perhaps?

Answer: Figure R7 shows the joint histogram of rCRE and LWP. This figure will be included in the Supplementary section of the manuscript.

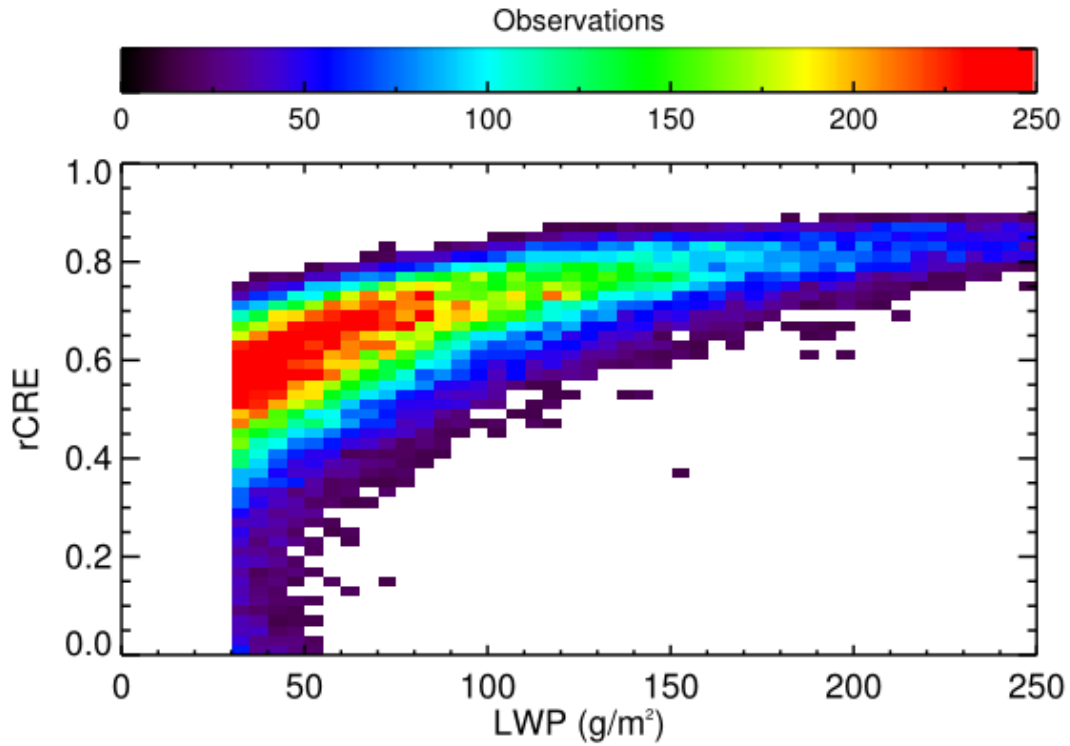


Figure R7: Joint histogram of rCRE and LWP.

p32 Figure 9d: one more tick mark on the x-axis to properly define it.

Answer: Done.

A long-term study of aerosol-cloud interactions and their radiative effect at ~~a mid-latitude continental site~~ the Southern Great Plains using ground-based measurements

Elisa T. Sena^{1,2}, Allison McComiskey³, and Graham Feingold²

5 ¹Institute of Physics, University of São Paulo, São Paulo, Brazil

²NOAA Chemical Sciences Division, Boulder, CO

³NOAA Global Monitoring Division, Boulder, CO

Correspondence to: Elisa T. Sena (elisa.sena@noaa.gov)

Abstract. Empirical estimates of the microphysical response of cloud droplet size distribution to aerosol perturbations are commonly used to constrain aerosol-cloud interactions in climate models. Instead of empirical microphysical estimates, here macroscopic variables are analyzed to address the influences of aerosol particles and meteorological descriptors on instantaneous cloud albedo and the radiative effect of shallow liquid water clouds. Long-term ground-based measurements from the Atmospheric Radiation Measurement (ARM) Program over the Southern Great Plains are used. A broad statistical analysis was performed on 14-years of coincident measurements of low clouds, aerosol, and meteorological properties. Two cases representing conflicting results regarding the relationship between the aerosol and the cloud radiative effect were selected and studied in greater detail. Microphysical estimates are shown to be very uncertain and to depend strongly on the methodology, retrieval technique, and averaging scale. For this continental site, the results indicate that the influence of the aerosol on the shallow cloud radiative effect and albedo is weak and that macroscopic cloud properties and dynamics play a much larger role in determining the instantaneous cloud radiative effect compared to microphysical effects. On a daily basis, aerosol shows no correlation with cloud radiative properties (correlation = -0.01 ± 0.03) whereas liquid water path shows a clear signal (correlation = 0.56 ± 0.02).

10
15
20

1 Introduction

Clouds are major contributors to global reflectivity (Trenberth et al., 2009). Thus, changes in cloud albedo, coverage, and lifetime have a large impact on the Earth's radiation budget. Additionally, changes in precipitation patterns may have a large impact on agriculture, the environment, and human well-being.

25

The influence of aerosol on clouds and its contribution to cloud radiative forcing has become a theme of much debate in the scientific community (Boucher et al., 2013). The processes involved in cloud development, aerosol and cloud lifecycles, and cloud radiative responses are complex and not well represented in global climate models (GCMs). Microphysical responses associated with aerosol effects on cloud albedo ~~follow the~~ tend to be described as a sequence of more aerosol resulting in

more cloud condensation nuclei (CCN), and all else equal, smaller cloud drops and a more reflective cloud (Twomey 1974, 1977). However, aerosol, dynamics and macroscopic cloud properties are interconnected, and may result in mutually compensating effects and adjustments that are not fully understood (Stevens and Feingold, 2009). For example, smaller drops may suppress precipitation and increase cloudiness (Albrecht, 1989) or, by enhancing entrainment and evaporation, decrease cloud amount (Wang et al. 2003; Ackerman et al. 2004; Small et al. 2009). Absorbing aerosol could also modify the atmospheric temperature profile and stability, and reduce cloud amount via the semi-direct effect (e.g., [Huang et al., 2009](#), [Koren et al., 2008](#); [Huang et al., 2009](#)).

Therefore, cloud microphysical variations do not necessarily manifest as changes in cloud albedo and radiative forcing (Han et al., 1998). The influence of [meteorological drivers and thermodynamic conditions \(e.g., atmospheric stability and humidity\)](#) on aerosol-cloud interaction assessments is increasingly being brought into focus (e.g., [Engstrom and Eekman, 2010](#), Kaufman, et al., 2005, [Engstrom and Eckman, 2010](#), Koren et al., 2012, Chen et al., 2014, Chen et al., 2015). However, untangling the cloud microphysical effects from dynamics and isolating their contributions to the radiative balance still remains a big challenge. Direct, independent, and collocated measurements of each pertinent variable are required for understanding the impact of the anthropogenic aerosol on the cloud radiative effect (McComiskey and Feingold, 2012).

Evidence for anthropogenic aerosol influence on cloud droplet number concentration and effective radius is commonly ~~seen~~ [from noted in](#) *in situ* airborne measurements (e.g., Warner and Twomey, 1967, Eagan et al., 1974, Ackerman et al., 2000, Twohy et al., 2005). Over the past two decades, satellite remote sensing has been widely used to study aerosol-cloud interactions over large areas (e.g., Nakajima et al., 2001, Bréon et al., 2002, Quaas et al., 2008, Costantino and Bréon, 2010), usually showing weaker responses than airborne-based studies. Space-borne assessments of aerosol-cloud interactions face many challenges, such as cloud contamination of the aerosol measurement, aerosol humidification effects near clouds, and the difficulty in obtaining collocated aerosol and cloud measurements. Different observational scales and platforms result in large variations in the aerosol-cloud interaction assessments (McComiskey and Feingold, 2012).

The Department of Energy's (DOE) Atmospheric Radiation Measurement (ARM) Program continuously operates permanent and mobile facilities that allow monitoring and ~~studying~~ [study of](#) the atmosphere at different sites. The unrivaled combination of in-situ and ground-based remote sensing instruments provides collocated and simultaneous measurements of different cloud, aerosol and meteorological properties. ARM ground-based instrumentation has been previously used to study aerosol-cloud interactions at several sites around the world (e.g., Feingold et al., 2003, Kim et al., 2003, [Garrett et al., 2004](#), Kim et al., 2008, McComiskey et al., 2009, [Garrett et al., 2004](#)). These studies focused on the microphysical aspect of aerosol-cloud interaction, analyzing a handful, to months, to up to three years of measurements. The ARM Program has been operating at the Southern Great Plains (SGP), Oklahoma, for more than two decades (since 1992). The availability of such a large and comprehensive dataset provides an excellent opportunity to pursue a long-term study of the effects of aerosol and meteorology on clouds.

In this work, 14-years of ARM ground-based measurements at the SGP were analyzed to investigate the effects of aerosol and [meteorological drivers \(such as capping inversion strength, surface-boundary layer coupling and turbulence\)](#)

meteorology on clouds. Instead of quantifying the usual metrics for microphysical response to an aerosol perturbation, we focus on the analysis of aerosol associations with cloud macroscopic variables and radiative properties. These quantities are more closely related to the cloud radiative effect and therefore represent a pragmatic pathway towards quantification.

The structure of the paper is as follows: Section 2 describes the methodology. A climatology of low, warm, non-precipitating clouds at the SGP is then presented (Section 3.1). Some simple approximations are used to illustrate the theoretical basis behind the data analysis (Section 3.2). A broad statistical analysis of more than a decade of coincident ground-based measurements of cloud radiative properties and their relationship with meteorology and aerosol concentration is shown (Section 3.3). Two interesting cases are selected and studied more deeply to improve our understanding of the problem (Section 3.4). Common features observed in the case studies are further explored (Section 3.5). We summarize our results in Section 4.

2 Methodology

Coincident ground-based remote sensing and in-situ measurements of clouds, aerosol and meteorological properties from Atmospheric Radiation Measurement (ARM) deployments at the Southern Great Plains (SGP), Central Facility, near Lamont, Oklahoma (36.61°N, 97.48°W), were used. The period of data analysis ranges from 1997 to 2010 and includes all available data that present coincident measurements of the variables considered, subject to the restrictions described below.

The Active Remotely Sensed Cloud Locations (ARSCL) Value-Added Product (Clothiaux et al., 2000) was used to select low, warm, non-precipitating clouds from the full 14 years of data. This product combines measurements from a Ka-band cloud radar (35 GHz or 8.6 mm wavelength), a ceilometer at a wavelength of 910 nm, and a Micropulse Lidar (MPL) at 532 nm to provide, among other variables, best estimates of cloud boundaries at 10-second resolution. To avoid ice, the cloud base height h_{CB} was limited between 300 m and 2000 m and the cloud top h_{CT} was limited to 3000 m. Cases that presented more than one layer of cloud were excluded from the analysis. Drizzle was mostly avoided by limiting the maximum column radar reflectivity (Z) to less than -17 dBZ (Frisch et al., 1995).

Surface broadband shortwave radiative fluxes were used to obtain cloud optical depth τ_c , (a parameter closely related to cloud albedo, A_c), cloud fraction f_c , and the instantaneous relative cloud radiative forcing rCRE, using the Radiative Flux Analysis Evaluation Product (RFA, Barnard and Long, 2004, Long and Ackerman, 2000, Long and Shi, 2006, Long et al., 2006). Overcast conditions ($f_c > 0.95$ on the scale of hundreds of meters) and solar zenith angle smaller than 80 degrees are required to retrieve τ_c . Parameters A_c and f_c were simultaneously retrieved using piecewise polynomial fits to functions of shortwave upward and downward radiation fluxes (Liu et al., 2011; Xie and Liu, 2013). rCRE, a non-dimensional measure of instantaneous cloud radiative forcing, or cloud radiative effect (Betts and Vittorbo, 2005) is defined as

$$rCRE = 1 - \frac{F_{all}^{dn}}{F_{clr}^{dn}}, \quad (1)$$

where F_{all}^{dn} and F_{clr}^{dn} are the broadband all-sky and clear-sky surface downwelling shortwave radiative fluxes (from 0.3 to 3.0 μm), respectively. The use of downwelling fluxes as opposed to net fluxes minimizes the effects of surface albedo on rCRE (Vavrus, 2006).

The aerosol index A_i was calculated from the surface scattering coefficient at 550 nm (σ_{550nm}) multiplied by the Ångström exponent (Å) and used as a proxy for CCN concentration (Nakajima et al., 2001)

$$A_i = \sigma_{550nm} \text{Å}, \quad (2)$$

where Å and σ_{550nm} were measured by a 3-channel nephelometer (at 450, 550 and 700 nm) at 1-minute resolution (Sheridan et al., 2001). An impactor at the inlet connected to the nephelometer alternates the cut size from 1 to 10 μm every 6 minutes.

Only measurements obtained at the 1- μm size cut were selected. The data were interpolated to 1-minute resolution, when necessary. The decision to use surface measurements is both pragmatic (they are available) but also supported by the result that at SGP the relationship between surface aerosol measurements and cloud level aerosol measurements has been shown to

be uncorrelated with the degree of boundary layer vertical mixing (Delle Monache et al. 2004). Their work shows that, at SGP, extensive and intensive aerosol properties measured at the surface and within the atmospheric boundary layer -are well-correlated. Therefore surface-based measurements of aerosol properties are representative of the air within the atmospheric boundary-layer. They also show that this finding does not depend on the mixing state of the atmosphere. Further analysis presented below confirms that our main results are only weakly dependent on the degree of mixing (Fig. 6). Another proxy for CCN was also used and showed similar results to those obtained using A_i (see Fig. S1 in the supplementary section).

Liquid water path (LWP) retrievals from a 2-channel (23.8 and 31.4 GHz) microwave radiometer (MWR) at 20-second resolution (Turner et al., 2007a) were used. Two different LWP ranges were selected. In the first part of this work (Section 3.3), our goal is to understand how several different properties impact rCRE. For ~~that-this~~ part of the study, LWP is limited between 30 and 250 g m^{-2} , allowing us to include cloud types ranging from low liquid water clouds (Vogelmann et al, 2012, Turner et al., 2007b), some of which are likely broken, to thicker, possibly drizzling clouds. The lower limit was set taking into account the large uncertainty in the MWR retrieval for low LWP. For the remaining analysis LWP was further restricted from 50 to 150 g m^{-2} . ~~This-The~~ larger restriction to the upper range was applied to minimize contributions from precipitating events. The increased lower limit avoids very thin or broken clouds where the uncertainty in measuring LWP is high (Turner et al., 2007b).

Turbulence, via its influence on supersaturation, plays an important role in determining the number concentration of aerosol particles that are activated to become cloud droplets (e.g., Twomey, 1959, Feingold et al., 2003). The vertical component of the turbulent kinetic energy provides an estimate of the strength of the turbulent fluxes acting at cloud base. Doppler radar vertical velocities were used to calculate a proxy for turbulence given by $w'^2 = [w - w_0]^2$, where w is the Doppler radar vertical velocity at the cloud base, and w_0 is the average vertical velocity at the cloud base centered ± 30 min around each measurement.

The decoupling index D_i is an indicator of how well-mixed the atmosphere is, and therefore how well ground-based measurements of conserved variables and aerosol properties represent the same at cloud base:

$$D_i = \frac{h_{CB} - LCL}{h_{CB}}, \quad (3)$$

where the lifting condensation level (LCL) is calculated using ground-based meteorological measurements of surface pressure, vapor mixing ratio, and temperature. As [the](#) D_i retrieval depends on h_{CB} it can only be calculated in the presence of a cloud. This means that D_i does not necessarily reflect the mean mixing state, unless f_c is high. In broken cloud scenes, a cloud element may be well coupled, whereas the average for the entire boundary layer may be poorly coupled. This should be kept in mind in subsequent discussion.

The lower tropospheric stability (LTS), given by the difference between potential temperatures at 700 hPa and at the surface, was also analyzed. This variable is related to the strength of the capping inversion. Studies show that LTS correlates well with the f_c of low stratiform clouds ([Chen et al., 2014](#), Klein and Hartmann, 1993; [Chen et al., 2014](#)). The potential temperatures were obtained from the Merged Sounding Value-Added Product (Trojan, 2012), version 1. This product combines radiosondes, MWR, surface measurements and the European Centre for Medium Range Weather Forecasts (ECMWF) model output to provide several relevant meteorological parameters at 1-minute resolution, at 266 pressure levels, up to 20 km.

A summary of the instruments, the temporal resolution in the original data set, measurements and retrievals used in this work is shown in Table 1. All of the relevant variables were averaged (or interpolated, in case of A_i) to 1-minute resolution for the analyses presented here.

3 Results

3.1 Database characterization

A statistical analysis of the data set used in this study is performed. Relative frequency histograms show the distribution of some of the key properties that ~~satisfied~~ satisfy the selection criteria explained in the previous section (Fig. 1). Red bars represent the distribution obtained when LWP is limited between 30 and 250 g m⁻²; the blue bars are obtained by limiting LWP between 50 and 150 g m⁻². The mean (dot), median (cross) and standard deviation (vertical lines) are shown above each distribution. The data set represents about ~~66,000~~ 39,000 valid observations for the first criterion (~~bluered~~) and about ~~39,000~~ 66,000 for the second criterion (~~redblue~~). Due to the long duration of this study period, these distributions can be regarded as representative of low-level, warm, non-precipitating clouds at the SGP for the selection criteria stated above.

Figure 1a shows that the data are dominated by clouds with lower LWP, with the number of observations decreasing as LWP increases. The more restrictive LWP limit (blue bars) shows a higher relative frequency than the less restrictive limit (red bars), due to the smaller number of observations. The non-cloud properties are barely affected by changing the LWP limits.

For A_i , D_i , LTS and w'^2 (Fig. 1i-l) the red and blue distributions are essentially the same. On the other hand, the distributions

of most of the cloud properties are modified depending on the LWP limit considered. A_c , cloud thickness, τ_c , rCRE and f_c show a narrower distribution when the LWP range is restricted (Fig. 1c-f), indicating that these variables are closely related to LWP (Turner et al., 2007b).

Due to our selection criteria (low, warm, non-precipitating clouds), most of the data represent stratiform clouds, characterized by high f_c . Figure 1b shows that about 92% of the observations were acquired in overcast conditions (f_c greater than 0.9). The number of broken-cloud observations ($f_c < 0.9$) ~~are-is~~ about 6800 and 3300 for the less and more restrictive LWP ranges, respectively. The fraction of data points with $f_c > 0.99$ is 79%, for LWP between 50 and 150 g m^{-2} and 75% for LWP between 30 and 250 g m^{-2} .

To a good approximation, rCRE is directly proportional to both A_c and f_c (Xie and Liu, 2013):

$$rCRE \sim f_c A_c. \quad (4)$$

As most of the observations were obtained in overcast conditions (Fig. 1b), rCRE in this study is mostly determined by A_c , and therefore the shapes of the distributions of rCRE and A_c (Fig. 1c-d) are very similar (slightly negatively skewed). Due to the polynomial criterion used to calculate A_c , about 0.5% of the observations resulted in $A_c = 0$. The median values obtained for rCRE, A_c and τ_c (Fig. 1c-e) were about 0.68, 0.62 and 17, respectively, for the more restrictive LWP range, and about 2 to 3% smaller when the LWP restriction was relaxed.

As expected, the A_i distribution (Fig. 1i) is positively skewed indicating the predominance of clean cases (low A_i) over polluted cases. The distribution of the turbulence proxy (w'^2) peaks at 0 and rapidly decreases as w'^2 increases. This is due to the small number of cumulus observations in the database, which are usually associated with higher turbulent fluxes. For about one-third of the observations, w'^2 is ~~higher-greater~~ than 0.1.

Most of the selected clouds can be classified as thin clouds (Fig. 1f). About 54% of the observations correspond to clouds thinner than 500 m, with cloud thickness peaking at about 300 m. Almost 70% of the cases correspond to clouds with h_{CB} lower than 1 km, and for more than 82% of the cases, h_{CT} is lower than 2 km.

By definition (Eq. 3) a value of $D_i = 0$ represents a well-mixed boundary layer whereas values greater than 0 represent progressively more decoupled boundary layers and therefore progressively weaker vertical mixing. The median of the D_i distribution (Fig. 1k) is about 0.37, and about 31% of the observations show significant decoupling with D_i larger than 0.5.

The few cases of negative D_i shown in this distribution are most likely attributed to incorrect retrievals of the h_{CB} . The LTS distribution (Fig. 1l) is roughly symmetrical and varies between 9 and 20 K, within one standard deviation. These LTS values are smaller than a previously published long-term evaluation (2001 – 2010) that reported a mean value of 20.81 K for stratiform cloud LTSs at SGP (Ghate et al., 2015), based on 83 radiosonde soundings obtained between 2001 and 2010, for both, nighttime and daytime. A low bias in the LTS from the merged sonde product can be expected because of the inherent smoothing of the merged soundings used in this work.

Notwithstanding the important role of f_c in cloud radiative effect (Eq. 4), the predominance of high f_c in this data set shifts our attention in the following analysis to the relationships amongst rCRE, A_c , τ_c , LWP, and A_i .

3.2 Theoretical basis

For high f_c conditions, cloud liquid water is an important driver of variability in cloud radiative effect because it is so tightly correlated with τ_c and A_c (e.g., [Han et al., 1998](#), Kim et al. 2003; ~~[Han et al., 1998](#)~~, Chen et al., 2014). Thus, we are particularly interested in the relationship between rCRE and LWP and, by contrast, the relationship between rCRE and aerosol. To give us some insight into the expected behavior of this function, a simple theoretical relation is derived.

The rCRE (Eq. 1), can be expressed as

$$rCRE = 1 - T, \quad (5)$$

where T is the total cloud transmissivity.

Considering conservative cloud scattering (that is, no absorption), T is obtained using a two-stream radiative transfer approximation (Bohren, 1987) given by:

$$T = \frac{2\cos\theta_0}{2 + \frac{(1-g)\tau_c}{\cos\theta_0}}, \quad (6)$$

where g represents the asymmetry parameter of the cloud droplets and θ_0 is the solar zenith angle. This same two-stream approximation yields

$$A_c = \frac{\frac{(1-g)\tau_c}{\cos\theta_0}}{2 + \frac{(1-g)\tau_c}{\cos\theta_0}}. \quad (7)$$

Replacing T (Eq. 6) in Equation 5 and performing some algebraic manipulations, the rCRE can be expressed as a function of τ_c :

$$rCRE = \left[1 + \frac{2\cos\theta_0}{(1-g)\tau_c} \right]^{-1}. \quad (8)$$

Equation 8 shows that, for fixed illumination angle and cloud scattering geometry, rCRE increases with τ_c .

In the adiabatic regime, τ_c relates to cloud droplet concentration (N_d) and LWP through (Boers and Mitchell, 1994)

$$\tau_c = c(T, p) N_d^{\frac{1}{3}} LWP^{\frac{5}{6}}, \quad (9)$$

where $c(T, p)$ is a known function of temperature T and pressure p . According to Eq. 9, the LWP contribution to τ_c is, in a relative sense, 2.5 times [larger than](#) that of N_d . The same can be shown to be true for sub-adiabatic clouds (Boers and Mitchell 1994). Note that in presenting these equations with respect to N_d we inherently assume a proportionality between N_d and aerosol concentration N_a (or proxy such as A_i). If τ_c were to be cast in terms of N_a , the power law dependence of τ_c on N_a would be less than 1/3. Because of the uncertainty in the relationship between N_d and N_a we use N_d to simplify the theoretical arguments.

τ_c (and therefore A_c) thus subsumes both the amount of condensed water, a macroscale property, as well as drop (or aerosol) concentration, a microphysical property. Thus ~~for a given~~ the extent to which the rCRE dependence on LWP differs for different aerosol concentrations is an expression of the importance of the aerosol in driving rCRE.

Using Equations 8 and 9, rCRE can be expressed as a function of LWP and N_d . The radiative susceptibility of a cloud to changes in N_d is given by:

$$\left. \frac{drCRE}{dN_d} = \frac{rCRE(1 - rCRE)}{3N_d} \right|_{LWP}. \quad (10)$$

Figure 2 shows examples of the theoretical relationships between rCRE and LWP, and between cloud radiative susceptibility and rCRE for different N_d : 200 cm^{-3} (blue), 500 cm^{-3} (red), and 1000 cm^{-3} (green). The mean solar zenith angle observed at ~~the~~-SGP ($\theta_0 = 45^\circ$) was used, and we assumed $g = 0.86$, $T = 300\text{K}$ and $p = 1000 \text{ mb}$.

Figure 2a shows that for lower LWP values rCRE increases rapidly with increasing LWP. The rate of increase decreases with progressive increase in LWP until the curve begins to saturate. In this example, the saturation begins for rCRE between around 0.7 to 0.8. Complete saturation does not occur at rCRE = 1 due to the diffuse component of the all-sky downwelling shortwave radiation flux. For a very optically thick cloud the direct beam is extinguished but the diffuse component is equal to the total radiation, assuring that the total radiation transmission does not vanish. Therefore, total radiation extinction does not occur as quickly as might be expected. We also observe a slight increase in rCRE with increasing N_d . The rCRE is more sensitive to changes in N_d at moderate LWP values (between 50 and 100 g m^{-2}). Also, for a fixed LWP, the difference between the rCRE obtained for $N_d = 200 \text{ cm}^{-3}$ and $N_d = 500 \text{ cm}^{-3}$ is larger than the rCRE difference obtained using the larger N_d ($N_d = 500 \text{ cm}^{-3}$ and $N_d = 1000 \text{ cm}^{-3}$). The maximum radiative susceptibility occurs at rCRE = 0.5, and is higher for smaller N_d (Fig. 2b). This is consistent with previous results that predict that cleaner clouds are more susceptible to A_c changes than polluted clouds (Platnick and Twomey, 1994). The same authors also report that A_c sensitivity to N_d is a maximum when A_c is 0.5, which is consistent with the larger separation between the curves in the moderate LWP range and for rCRE = 0.5.

3.3 Broad statistical analysis of the observations

To understand how the cloud radiative effect responds to changes in different parameters, a broad statistical analysis of the long-term dataset obtained at SGP was undertaken. As LWP largely dominates rCRE (Eqs. 8 and 9, Fig. 2), the data were binned by rCRE and LWP. The bin sizes were 0.02 for rCRE and 5 g m^{-2} for LWP. For each bin the average of several different variables (A_i , D_i , f_c , LTS, τ_c and w^2) was calculated. This procedure allows us to isolate the LWP contribution to rCRE and to observe the associations of other properties with rCRE in the third (colored) dimension. To reduce variability due to poor sampling statistics, we require at least 15 points in each 2D-bin. To observe the general trend of rCRE with LWP and the other variables, for this analysis, the broader LWP range was used. Solar zenith angle (θ_0) was limited to 80 degrees to avoid errors in the cloud properties retrieved from the shortwave broadband radiative fluxes. The joint frequency distribution of rCRE and LWP for this data set is shown in the supplement (Fig. S2).

Figure 3 shows that rCRE presents a clear increasing tendency with LWP, in agreement with the theoretical two-stream approximation, shown in Figure 2. ~~ies. Because the data set is dominated by $f_c \rightarrow 1$, for a fixed LWP, differences in rCRE are primarily due to microphysical influences. The distribution of LWP (Fig. 1a) indicates that the number of observations decreases with increasing LWP. The larger number of observations at lower LWP results in a larger vertical rCRE spread for~~
5 ~~the low LWP values, compared to the high LWP. Several factors contribute to the variation of rCRE observed for a fixed LWP. According to Equation (8), rCRE increases with solar zenith angle (θ_0). Therefore for a fixed LWP, differences in rCRE can be associated with different times of the day, and day of the year.~~ Some rCRE differences could be related to the relatively small number of broken cloud events that: i) reduce rCRE due to the smaller f_c associated with this cloud type; and, ii) introduce the possibility of three-dimensional radiative effects (e.g., Wen et al. 2007) ~~or other retrieval errors, and therefore deviations from the simple two-stream model approximations that form the basis of the rCRE analysis, and therefore deviations from the simple two stream model approximations that form the basis of the rCRE analysis. The distribution of LWP (Fig. 1a) indicates that the number of observations decreases with increasing LWP. Therefore, the larger number of observations at lower LWP results in a larger rCRE spread for low LWP values, compared to the high LWP. This~~ further contributes to the vertical spread of points at low LWP.

15 For the liquid clouds that meet our analysis criteria, two different cloud types are identified: i) broken-cumulus clouds characterized by lower mean f_c and higher w'^2 , and ii) stratiform clouds -associated with higher f_c and lower w'^2 . As most broken cumuli are concentrated in the lowest LWP range (usually LWP < 100 g m⁻²) and have lower f_c , they generally present smaller rCREs than stratiform clouds (Eq. 4). ~~There are exceptions where lower f_c in the lowest LWP range present higher rCRE. This may be due to the deviation from the two-stream model because of three-dimensional radiative effects, or~~
20 ~~some aerosol-related effect on the cloud properties.~~ Since broken cumuli are associated with local convection it is expected that this type of cloud exhibits a higher local coupling with the surface, and therefore a smaller D_i , as observed in Figure 3d. On the other hand, the stratiform clouds at SGP tend to be associated with deeper boundary layers, therefore leading to higher decoupling between the surface and the atmosphere. Stratiform clouds are also controlled by large-scale subsidence and exhibit a higher LTS than broken cumuli (Fig. 3f). The joint probability distribution function of D_i and f_c shows that low
25 f_c cases are generally only observed when D_i is low (Fig. 4), with the exception of a few spurious data points.

Figure 3b shows the strong dependence of τ_c on LWP, in agreement with Equation (9). The dependence of rCRE on τ_c is also easily identified. As τ_c is only retrieved for $f_c > 0.95$, low rCRE values ~~are not observed~~ do not appear in Fig. 3b. For a fixed LWP, rCRE exhibits a weak trend with A_i (Fig. 3a). When LWP is smaller than about 100 g m⁻², this trend seems to occur in both directions, indicating that both high and low rCRE can be observed in more polluted conditions. One could infer that
30 the positive trend is due to cloud microphysical changes caused by higher aerosol loading, while the negative trend could be due to the semi-direct effect of aerosol on clouds. ~~(We found no evidence of significant aerosol absorption for these cases.)~~ However, meteorology also impacts the system and influences the rCRE. For example, different cloud dynamics could be linked to both changes in rCRE and in aerosol concentration. To understand the role that meteorology plays on the rCRE, some dynamical indices are now considered.

Higher turbulence facilitates more efficient droplet activation. Therefore, considering that for a constant LWP, variation in A_c is due to changes in N_d , it is expected that, more turbulence would result in more droplets and higher cloud radiative effect (Feingold et al., 2003). However, Figure 3c shows that for a fixed LWP there is a weak dependence of rCRE on w'^2 , with higher rCRE usually occurring for *weaker* turbulence. This result ~~suggests~~ ~~confirms~~ ~~indicate~~ ~~confirms~~ that in most cases the rCRE is more dependent on macroscale cloud properties such as LWP and f_c than on cloud microphysics. For example, in most cases higher turbulence is associated with broken cumuli that present lower f_c , and therefore lower rCRE.

The correlation coefficients between the mean f_c , LTS and D_i (Fig. 3d-f) were calculated. The correlation between f_c and D_i ($\rho_{f_c, D_i} = 0.72$) is larger than the correlation between f_c and LTS ($\rho_{f_c, LTS} = 0.55$). The correlation between LTS and D_i is also positive, with $\rho_{LTS, D_i} = 0.54$. As previously mentioned, LTS and f_c are expected to correlate well for low stratiform clouds. However, as the data in Figure 3 also include some broken clouds, $\rho_{f_c, LTS}$ is not as high as in previous assessments that only analyzed stratiform clouds (eg. Klein and Hartmann, 1993, Wood and Bretherton, 2006). We hypothesize that the stronger ρ_{f_c, D_i} compared to $\rho_{f_c, LTS}$ is a consequence of two factors: (i) D_i is calculated for each cloud element and is therefore closely connected to the local cloud conditions, and (ii) LTS is based on the potential temperature at 700 hPa, which may not always be relevant to the local cloud conditions.

Both meteorological indices used in the analysis, LTS and D_i , as well as f_c , (Fig. 3d-f) impart a ~~clearer~~ ~~less ambiguous~~ signal in rCRE than does A_i (Fig. 3a). Figures 3d-f show that, on average, the rCRE is larger for less coupled atmospheric conditions, higher LTS and higher f_c , associated with solid stratiform clouds. Figure 3e shows considerable f_c changes that dominate rCRE variability at low LWP. These results indicate confirm that the cloud radiative effect is more related to macroscopic variables such as LWP and f_c than to changes in aerosol loading and cloud microphysics. also suggest confirm that, in most cases, the cloud radiative effect is more closely related to cloud macroscopic variables are more related to the cloud radiative effect than to cloud microphysics. At low LWP and higher rCRE, we find lower cloud fractions, which could indeed indicate the predominance of a microphysical effect. Some higher turbulence values are found here along with moderate aerosol index, but unfortunately those data are somewhat not fully unambiguous and may suffer from three-dimensional radiative effects or other retrieval error.

The analysis performed in Figure 3 provides useful information regarding how rCRE relates to macroscopic cloud properties, aerosol, and meteorological indices. However, as observed in Equation (8), rCRE also depends on solar zenith angle (θ_0). In fact, rCRE varies slowly with θ_0 for lower θ_0 values, but shows a strong dependence on θ_0 for higher angles. This intrinsic dependence of rCRE on θ_0 does not allow us to isolate the effects on rCRE due solely to other properties on rCRE from the effects caused by solar illumination angle. To reduce this influence, only cases obtained when $\cos(\theta_0) \geq 0.6$ were considered for further analysis. This limit was selected such as to maximize the amount of data analyzed and at the same time, minimize the effects of θ_0 solar illumination on rCRE. Figure 5 shows rCRE as a function of LWP and the same variables analyzed in Figure 3, when $\cos(\theta_0) \geq 0.6$. We note a priori that this filter preferentially removes early morning

and late afternoon data, with more data loss in the wintertime. Whereas 18% of the observations in Fig. 3 were obtained during wintertime, due to the larger θ_0 restriction, for Fig. 5 this number is reduced to only 2% data.

Figure 5 shows that the general trends of rCRE with these variables do not change significantly for aerosol and τ_c , when θ_0 is limited. However, for D_i , f_c , w^2 , and LTS the rCRE trends at a fixed LWP value previously observed in these figures are reduced compared to Fig. 3. One of the explanations for this behavior is that, as these variables have a marked diurnal cycle, limiting θ_0 significantly reduces their variability. For example, higher D_i values are usually observed during early-morning and late-afternoon. Therefore when only low θ_0 values are considered, these higher D_i observations will not appear as frequently in the data set. On the other hand, as higher LWP values are associated with higher f_c , higher D_i and lower w^2 values, high rCRE values will likely be observed when these macroscopic properties and thermodynamic conditions are met. The diurnal cycle of D_i will be further discussed in Section 3.5. Besides these factors, as the data set is dominated by $f_c \sim 1$, for a fixed LWP and low θ_0 values, differences in rCRE should be dominated by microphysical influences. However, with the convolution of f_c and aerosol it is hard to definitively untangle these effects.

Cloud albedo was also analyzed as a function of LWP and the six other variables analyzed in Figures 3 and 5. However, as rCRE is directly proportional to the product of A_c and f_c (Eq. 4) and most of the observations are concentrated at the same cloud fraction bin (Fig. 1b), the results obtained for A_c are very similar to the ones obtained for rCRE and are therefore not shown here. To isolate the effects of f_c and A_c on rCRE, the variation of A_c with five key variables (LWP, A_i , w^2 , D_i and LTS) for completely overcast conditions ($f_c = 1$) was analysed (Fig. 6). For this analysis only cases observed when $\cos(\theta_0) \geq 0.6$ were considered. The joint distribution of these variables for this more restrictive data set is shown in the supplement (Fig. S3). Figure 6 shows that, for this more restrictive range of θ_0 , D_i and LTS have a stronger influence on A_c than does A_i . This implies that, besides their association with f_c , D_i and LTS also have a direct impact on A_c (and, in turn, on rCRE). On the other hand, for overcast conditions and $f_c = 1$, A_c does not show strong, systematic large variations with w^2 (Fig. 5b) neither any of these variables. For low LWP, there is a small amount number of points with high A_i and high A_c , which could be related to microphysical processes. It also seems that lower LWP values, associated with lower higher A_c are largely observed when stability is higher (high LTS), except where aerosol concentrations are highest. To really address the impact of these variables on A_c would require further detailed analysis of the high resolution data, rather than a broad statistical analysis, though and may be done in a which is deferred to future work. This suggests that the rCRE trend with w^2 observed in Figure 3c was really associated with the f_c variations observed in the different cloud regimes.

Since high f_c scenes dominate the data (Fig. 1b) and LWP plays a central role in cloud radiative responses, we attempted to identify and compare the signals due to LWP with those due to aerosol on rCRE. Daily correlations between rCRE and these two key variables (A_i and LWP) were analyzed. For this analysis, the LWP range was restricted to avoid drizzle and uncertain retrievals, as explained in section 3.2. Cases that had less than 25 points per day were excluded from this analysis. In the original database, 1093 days fit the low, warm, non-precipitating clouds criteria. After selecting cases that satisfied the minimum requisite number of points per day, low θ_0 ($\cos(\theta_0) \geq 0.6$), and had non-missing coincident retrievals of rCRE,

LWP and A_i , only ~~323-111~~ days remained. The histograms of the distribution of the correlations between rCRE and A_i (ρ_{rCRE,A_i}) and rCRE and LWP ($\rho_{rCRE,LWP}$) are shown in Figure 76.

~~According to~~ Figure 76a corroborates Figure 3a, showing that rCRE and A_i can either be positively or negatively correlated.

The proportion of negatively and positively correlated cases is roughly 50%/50% for ρ_{rCRE,A_i} . On the other hand, rCRE and

LWP show a much higher positive correlation than rCRE and A_i (Fig. 76b). The histograms show that ρ_{rCRE,A_i} is on average \pm

0.019 ± 0.032 while $\rho_{rCRE,LWP}$ was on average $0.460.56 \pm 0.02$. For about 980% of the cases rCRE and LWP are positively

correlated. Therefore we can infer that LWP clearly dominates the cloud radiative effect, while the aerosol signal on rCRE is

ambiguous. ~~A similar analysis was performed for more decoupled conditions ($D_i \geq 0.5$) and less decoupled conditions ($D_i \leq$~~

~~0.25) (Fig. 7). No significant differences were observed for different coupling conditions, supporting the result of Delle~~

~~Monache et al. (2004) that the relationship between surface aerosol measurements and cloud level aerosol measurements is~~

~~uncorrelated with the degree of boundary layer vertical mixing at this site.~~

3.4 Case studies

The results shown in the previous sections provide broad insight into the general macroscopic behavior observed for warm

clouds at SGP and the potential role of aerosol in driving this behavior. For a deeper understanding of the processes related

to those long-term trends, some cases were further analyzed. Two days that presented relatively high positive or negative

correlations between rCRE and A_i were selected and investigated further. The selected case studies have a long time series,

with at least 6 hours of rCRE retrievals, in addition to continuous measurements of relevant properties, providing a good

sample of observations.

3.4.1 Case study 1: Positive correlation between rCRE and A_i

Figure 8 shows the time series of several relevant measurements, such as τ_c , LWP, rCRE, A_i and D_i , for January 9th 2006.

The time series of the vertical profile of radar reflectivity (Z) is also shown. Since the rCRE can only be measured during

sunlit periods ($\theta_0 < 80^\circ$), this analysis focuses on that period. Due to the detection of multiple layers of clouds after 20 UTC,

the plots are restricted to the period from 12 to 20 UTC (6 to 14 LT). The correlation between rCRE and A_i for this day is

positive and about 0.75.

The radar reflectivity indicates that this case represents a solid stratiform cloud that begins to develop with the boundary

layer at ~ 12 UTC (Fig. 8b). h_{CT} peaks around 1 km and remains constant after 16 UTC. Note that according to the radar

reflectivity it is highly unlikely that this day was affected by precipitation.

The strong positive correlation between rCRE, τ_c and LWP is also noted (Fig. 8a). As previously pointed out these three

variables are closely related (Eqs. 8 and 9). On that day, radiometric measurements were only available after ~ 14 UTC, so

rCRE and τ_c were only retrieved after that time.

The increase in the incoming solar radiation absorbed by the atmosphere and reaching the surface, warms the atmosphere. The LCL increases with time until it stabilizes at 600 m around 18 UTC. The diurnal cycle of shortwave radiation affects the coupling between the surface and the boundary layer leading to more coupled conditions in the afternoon (Fig. 87d). The relation between D_i and solar radiation is further explored in sections 3.4.2 and 3.5.

5 After about 16h UTC both A_i and LWP, decrease (Fig. 8a). The mechanisms that lead to the decreases are most likely associated with entrainment and drying as the boundary layer deepens. (The relative humidity time series shows that [surface](#) RH decreases with time, until about 18 UTC, when it stabilizes at about 0.7). Dilution due to the increase in the boundary layer depth likely explains the drop in surface aerosol concentration and decrease in A_i .

Next, we aim to understand how the co-variability between LWP and A_i , could be linked to the response of rCRE to these two variables. Figure 9a-c shows the correlations between rCRE and A_i (ρ_{rCRE,A_i}), rCRE and LWP ($\rho_{rCRE,LWP}$) and LWP and A_i (ρ_{LWP,A_i}) for the selected day. Only points that have coincident measurements of all three variables – rCRE, LWP and A_i – are used. The number of valid points is 329.

For this day, all correlations are positive, with $\rho_{rCRE,A_i} = 0.75$, $\rho_{rCRE,LWP} = 0.82$ and $\rho_{LWP,A_i} = 0.50$. The results and theory shown in sections 3.2 and 3.3, indicate that the changes in LWP drive changes in rCRE. However, microphysical responses also need to be considered. For a vertically homogeneous cloud, r_e can be calculated as a function of LWP and the τ_c (Stephens, 1978).

$$r_e = 1.5 \frac{LWP}{\rho_w \tau_c}, \quad (11)$$

where LWP is given in g m^{-2} and r_e is given in μm and ρ_w is the density of liquid water in g cm^{-3} .

For a cloud with constant LWP, a measure of the strength of aerosol-cloud interaction (α) can be obtained from the relative change between droplet effective radius (r_e) and A_i :

$$\alpha = - \left. \frac{\partial \ln r_e}{\partial \ln A_i} \right|_{LWP}. \quad (12)$$

20 According to this definition, α is expected to be positive and vary between 0 and 0.33, with a typical value of 0.23 (Feingold et al., 2001, [McComiskey and Feingold, 2012](#)).

To assess the microphysical effect of aerosols on clouds, r_e was calculated using Equation 11 and plotted as a function of A_i . In an attempt to isolate the aerosol effects on r_e , the dataset was divided into three LWP bins. For each bin, the linear regression between the logarithm of r_e and logarithm of A_i , was obtained. The slope of each linear fit provides the parameter α (Fig. 9d).

For this case, r_e varied between 2 and 7 μm and α is positive, as expected. The values obtained for α are within the expected range, except for the higher LWP category (Fig. 9d). However, there is a large variability in the magnitude of α . For the highest LWP range, α is about twice the value obtained for the mid-range LWP.

The question remains whether the positive correlation between rCRE and A_i is a result of the positive correlation between rCRE and LWP observed on that and many days in this data set (Fig. 3) – i.e., a macrophysical response – or whether it is due to the negative correlation between r_e and A_i – i.e. a microphysical response. This single case study suggests that both contributions are possible, but raises concerns about being too reliant on the microphysical response as an indicator of aerosol-related rCRE.

3.4.2 Case study 2: Negative correlation between rCRE and A_i

A case that shows a high negative correlation between rCRE and A_i , April 26th 2006, was also selected and analyzed in detail. Similar to the previous case, Figure 10 shows the time series of some of the relevant measurements and retrievals for this day. As the cloud completely vanished during late afternoon the analysis timeframe was once again restricted to between 12 and 20 UTC. The radar profile is shown from earlier in the day (5 UTC and on), as some drizzle was detected during nighttime. The drizzle may have scavenged the aerosol particles and could explain the low A_i values shown in Figure 10c, through ~1450 UTC. The red line indicates daytime in Figure 10b.

Once again, a strong positive correlation between rCRE, τ_c and LWP is observed.

The evolution of D_i is similar to the previous case, indicating that for both days the coupling between atmosphere and surface is driven by the diurnal cycle of radiation, rather than by other variables. This day was much warmer than the previous case and presented higher LCL values and lower surface RH. The surface temperature differences between the two days varied from 6 K to 10 K during the period analyzed.

The temporal evolution of LWP and the vertical profile of reflectivity for April-26-2006 (Fig. 10b-c) indicate that at about 14 UTC the stratiform cloud begins to dissipate, transitioning to broken cumuli after ~17 UTC. The decrease in both LWP and f_c after 14h UTC coincides with an increase in A_i . One hypothesis to explain this behavior is that boundary layer deepening and entrainment drying reduce cloud amount as the day progresses. D_i decreases because when clouds do form (a prerequisite for calculating D_i) the local coupling is relatively strong. The increase in A_i from a low post-drizzle clean atmosphere could be a result of a combination of surface sources, transport, and entrainment of free tropospheric air. It is also possible that cloud breakup may be caused by the aerosol semi-direct effect, however A_i was lower on this day and the analysis of the Ångström exponent and single scattering albedo (SSA) indicate that there are no significant differences in aerosol intensive properties (and thus, perhaps in aerosol type) between this and the previous case. The mean Ångström exponent at 1 μm cut size for case 2 was 2.274 ± 0.010 , while in the previous case it was 2.107 ± 0.008 . The mean SSA was 0.9721 ± 0.0012 and 0.9826 ± 0.0004 , for case 2 and case 1, respectively. The difference in the uncertainty indicates that for case 2, both the Ångström exponent and SSA fluctuate more. Finally, while one might want to invoke a role for the increasing aerosol evaporating smaller droplets more efficiently, which in turn would decrease f_c (Small et al., 2009), these aerosol loadings are relatively low, and as already discussed in section 3.3, many other dynamical features influence f_c and cloud development, especially during the daytime.

The correlations between rCRE, LWP and A_i for case 2 are shown in Figure 11a-c. The microphysical effect of aerosol on drop size is shown in Figure 11d. The number of valid points for this study case is 204.

The correlation between rCRE and A_i is negative and equal to -0.65 for this case. The correlation between rCRE and LWP is 0.64, smaller than in the previous case study, but still positive, as expected. Figure 11c shows that for case 2, LWP and A_i are negatively correlated with $\rho_{LWP,A_i} = -0.44$.

The r_e retrievals indicate that the sizes of most of the droplets analyzed in this case fall in the same range as the previous case study (between 3 and 10 μm). Here, however, α is negative (Fig. 11d), for which there is no physical explanation given the stratification by LWP and our expectation that drop size decreases with an increasing number of CCN for the same amount of condensed water (Twomey, 1977). This unexpected behavior could derive from a combination of factors: uncertainty in measurements, uncertainty in linear fits, and possibly the rather broad LWP binning, among others. Given the unphysical r_e response to increasing aerosol, the positive correlation between rCRE and LWP, and the overwhelming contribution of macroscopic and dynamical variables to the cloud system compared to the aerosol signal discussed in section 3.3, the results indicate that the observed negative correlation between rCRE and A_i is most likely due to the fact that LWP and aerosol are negatively correlated, presumably due to independent factors.

Most techniques employed to retrieve τ_c using ground-based instruments rely on overcast conditions (eg., Barnard et al., 2008, Min and Harrison, 1996). Xie and Liu's (2013) technique can be used to retrieve τ_c for lower cloud coverage. In Figures 9d and 11d, r_e was calculated using retrievals of τ_c from a broadband radiometer (RFA) following Barnard and Long (2004). Additionally, two other methods were used to retrieve τ_c and r_e for the case studies highlighted above: the Multi-Filter Rotating Shadowband Radiometer (MFRSR, Turner and Min, 2004) and broadband radiometer retrievals by Xie and Liu (2013). Effective radii r_e , determined from the measured LWP and each of the τ_c retrievals, were used to obtain the aerosol-cloud interaction (α) slope (Table 2). Retrievals acquired when $\theta_0 > 70^\circ$ were excluded from this analysis as the measurements are less reliable at higher solar zenith angles and the retrievals diverged greatly at high θ_0 in some cases. The different methodologies used to retrieve τ_c result in different α , and, for some cases, even the sign of the slopes disagree. The difference observed for ~~α_{LWP}~~ α_{RFA} estimates shown in Table 2 compared to Figures 9 and 11, is due to the restriction of co-location of data points among the three datasets and the $\theta_0 < 70^\circ$ threshold.

As emphasized above, this comparison raises concerns about reliance on α ~~alone~~ ~~to~~ quantify aerosol-related rCRE in terms of microphysical metrics. The requirement of binning by LWP leaves low statistics for calculating slopes in each bin and uncertainties in the slopes are high. Given the low statistics, differences in the retrievals can result in the large differences in α seen here, including changes in sign. These microphysical measures are useful for detecting aerosol effects on cloud properties, but are best used in conjunction with other measurements to fully understand the relevant physical processes. Using these measures for- quantification of the aerosol indirect effect (the aerosol induced cloud radiative effect), especially in case studies where statistics are low, can be misleading. Studies that provide larger statistics may produce more

meaningful quantifications (e.g., McComiskey et al. 2009), but will still contain biases inherent in any retrievals used to provide input properties to the calculation.

3.5 Further generalizations

The diurnal cycles of the D_i , shown in two case studies of section 3.4, were very similar, with higher D_i in the morning and lower D_i around 20 UTC (Figs. 8d and 10d). To verify if this trend is generally observed, the complete time series obtained during this 14-year study was used. The dataset was divided into 0.5-hour bins and the mean diurnal cycle of D_i during daytime was analyzed (Fig. 12).

Figure 12 shows that the temporal evolution of D_i is strongly linked to the diurnal cycle of solar radiation. On average, the atmosphere is highly decoupled in the morning. As the sun rises, the surface gets warmer, and solar energy is transferred from the surface to the atmosphere, favoring more coupled conditions (lower D_i). The higher coupling between the surface and the atmosphere increases turbulence. As the incoming solar radiation during the afternoon decreases, the atmosphere gradually cools. After ~ 20 UTC, the boundary layer collapses leading to less coupled conditions in the late afternoon.

The results shown in the previous section also indicate that, for these two case studies, the correlation between rCRE and A_i has the same sign as the correlation between LWP and A_i (Figs. 9 and 11). For the first case study, ρ_{rCRE,A_i} and ρ_{LWP,A_i} is positive, while for the second case study both correlations are negative. This suggests that the sign of ρ_{rCRE,A_i} is mainly determined by ρ_{LWP,A_i} . We now test the validity of this hypothesis and if this statement can be expanded for the whole dataset. For each day the correlation between rCRE and A_i (ρ_{rCRE,A_i}) and between LWP and A_i (ρ_{LWP,A_i}) were calculated.

Figure 13 shows the results obtained for these correlations, where each point represents one day. This was done for the ~~323~~ 111 days that had coincident measurements of the three variables (A_i , LWP, and rCRE) at low θ_0 . An orthogonal linear fit of the observations was performed.

Figure 13 shows that this statement can be generalized. Usually, if A_i and LWP are positively (negatively) correlated, the correlation between rCRE and A_i is positive (negative). This relationship was further analyzed as a function of several variables (A_i , LWP, D_i , τ_c , wind direction, wind speed, surface RH, w^2), none of which significantly influenced the results.

Considering all the days analyzed, the correlation between ρ_{rCRE,A_i} and ρ_{LWP,A_i} is 0.540.71. Even when θ_0 is not restricted, and therefore variations in θ_0 might obscure this relationship, the correlation between ρ_{rCRE,A_i} and ρ_{LWP,A_i} is still large: -0.54. This result suggests that the aerosol signal observed in rCRE based on daily correlations may often be a misinterpretation of the positive relationship between rCRE and LWP. Once again, for the data set analyzed, which consists overwhelmingly of high f_c events, the cloud radiative effect appears to be predominantly driven by macroscopic variables rather than by microphysical responses.

Given the uncertainty in calculations of α (Table2) the current work sounds a cautionary note regarding placing too much emphasis on microphysical metrics. This does not exclude the possibility of an aerosol influence on the cloud radiative effect but suggests that careful analysis should be done to quantify macrophysical relationships, such as those shown here.

Moreover, consideration of the co-variability in aerosol and ~~meteorological conditions~~ cloud macroscopic quantities (LWP in particular) has a strong influence on the detectability of aerosol-induced rCRE and therefore deserves attention (George and Wood 2010; Feingold et al. 2016).

4 Summary and conclusions

5 | A comprehensive study was performed to understand the relative effects of aerosols, macroscopic cloud properties and meteorological drivers on the radiative effect of low-level clouds. Fourteen years of coincident ground-based clouds, aerosol and meteorological measurements over the SGP were analyzed. The impact of different physical properties on the instantaneous cloud radiative effect was studied. The dataset was divided into rCRE and LWP bins and the mean values of properties such as f_c , τ_c , D_i , LTS, A_i and turbulence were analyzed. Most of the data are characterized by high f_c so that rCRE is predominantly a function of A_c (Eq. 4), which is in turn a strong function of LWP, and to a lesser extent drop concentration (Eqs. 7 and 9). Whereas a strong dependence of rCRE on LWP is clearly identified, the average over the whole dataset shows ~~a weak an ambiguous~~ influence of aerosol on rCRE. For low LWP, polluted conditions are associated with both high and low rCRE. ~~The impact of LTS, and D_i , on rCRE is also stronger than the impact due to aerosol particles.~~ Since LWP is such a key driver of rCRE, the impact of the aerosols and of LWP on the cloud radiative effect were compared by assessing the daily correlations between rCRE and A_i and rCRE and LWP. While the daily distribution of $\rho_{CRE,LWP}$ shows a clear positive signal, the daily distribution of ρ_{rCRE,A_i} is centred around 0, confirming the previous statement that high aerosol concentrations can be associated with both higher and lower rCRE.

Case studies that showed both positive and negative correlations between rCRE and A_i were further investigated. For these two selected days, rCRE was positively (negatively) correlated with A_i when A_i and LWP were positively (negatively) correlated. This behavior can be generalized to the other days analyzed. The case studies also show that microphysical metrics to estimate aerosol-cloud interaction (Eq. 10) are very uncertain and reliance on these estimates to quantify aerosol-related rCRE can be misleading.

The diurnal cycle of D_i over the SGP is strongly driven by the diurnal cycle of solar radiation. Both, LTS and D_i are highly correlated with f_c however ρ_{f_c,D_i} is larger than $\rho_{f_c,LTS}$. This is because LTS and f_c are tightly related for stratiform cloud, but less so for broken clouds. On the other hand, D_i represents both cloud types well because it is calculated for individual cloud elements. Stratiform clouds are usually observed early in the morning, when the boundary layer is less coupled due to the smaller sensible heat flux. As the surface warms up, turbulence and therefore surface-atmosphere coupling increases, and broken cumuli that have smaller f_c are formed.

The results presented here indicate that to first order, macroscopic variables such as cloud condensate and f_c rather than cloud microphysics are the properties that most determine the cloud radiative effect. Clearly the aerosol can play a role by modifying drop size and influencing how LWP manifests in τ_c and A_c . However, while LWP and f_c present a clear signature on rCRE, the aerosol signal is barely distinguishable. The aerosol signal is also difficult to quantify because of the

uncertainty in calculation of the metrics derived from different methods (Table 2, Figs. 9d and 11d) and platforms (McComiskey and Feingold 2012). Future studies that focus on understanding the role of dynamics and other meteorological drivers that potentially alter the macroscopic cloud properties will be reported on in the near future.

Acknowledgements

- 5 The authors would like to thank the ARM (Atmospheric Radiation Measurement) Program for processing and providing the data sets used in this work. This work was supported by FAPESP grants 2014/04181-2 and 2013/08582-9, the U.S. Department of Energy's Atmospheric System Research (ASR) program by Grant DE-SC0014568 and by NOAA.

References

- 10 Ackerman, A. S., Toon, O. B., Taylor, J. P., Johnson, D. W., Hobbs, P. V., and Ferek, R. J.: Effects of aerosols on cloud albedo: Evaluation of Twomey's parameterization of cloud susceptibility using measurements of ship tracks, [Journal of the Atmospheric Sciences](#), 57(16), 2684-2695, 2000.
- Albrecht, B. A.: Aerosols, cloud microphysics, and fractional cloudiness, *Science*, 245(4923), 1227-1230, 1989.
- Barnard, J. C., and Long, C. N.: A simple empirical equation to calculate cloud optical thickness using shortwave broadband measurements, [Journal of applied meteorology](#), 43(7), 1057-1066, 2004.
- 15 Barnard, J. C., Long, C. N., Kassianov, E. I., McFarlane, S. A., Comstock, J. M., Freer, M., and McFarquhar, G. M.: Development and evaluation of a simple algorithm to find cloud optical depth with emphasis on thin ice clouds, *Open Atmos. Sci. J.*, 2, 46-55, 2008.
- Betts, A. K., and Viterbo, P.: Land-surface, boundary layer, and cloud-field coupling over the southwestern Amazon in ERA-40, [Journal of Geophysical Research: Atmospheres](#), 110(D14), 20058.
- 20 Boers, R., and Mitchell, R. M.: Absorption feedback in stratocumulus clouds influence on cloud top albedo, *Tellus A*, 46(3), 229-241, 1994.
- Bohren, C. F.: Multiple scattering of light and some of its observable consequences, *Am. J. Phys.*, 55.6, 524-533, 1987.
- Boucher, O., Randall, D., Artaxo, P., Bretherton, C., Feingold, G., Forster, P., Kerminen, V.-M., Kondo, Y., Liao, H., Lohmann, U., Rasch, P., Satheesh, S.K., Sherwood, S., Stevens, B. and Zhang, X. Y.: Clouds and aerosols. In *Climate change 2013: the physical science basis - Contribution of Working Group I to the Fifth Assessment Report of the Intergovernmental Panel on Climate Change*, 571-657, Cambridge University Press, 2013.
- 25 Bréon, F. M., Tanré D., and Generoso S.: Aerosol effect on cloud droplet size monitored from satellite, *Science*, 295(5556), 834-838, 2002.
- 30 [Brückner, M., Pospichal, B., Macke, A. and Wendisch, M.: A new multispectral cloud retrieval method for ship-based solar transmissivity measurements. J. Geophys. Res., 119\(19\), 2014.](#)

- Chen, Y. C., Christensen, M. W., Stephens, G. L., and Seinfeld, J. H.: Satellite-based estimate of global aerosol-cloud radiative forcing by marine warm clouds, *Nature Geoscience*, 7(9), 643-646, 2014.
- Chen, Y. C., Christensen, M. W., Diner, D. J., and Garay, M. J.: Aerosol-cloud interactions in ship tracks using Terra MODIS/MISR. ~~Journal of Geophysical Research: Atmospheres~~J. Geophys. Res., 120(7), 2819-2833, 2015.
- 5 Clothiaux, E., Ackerman, T., Mace, G., Moran, K., Marchand, R., Miller, M. and Martner, B.: Objective determination of cloud heights and radar reflectivities using a combination of active remote sensors at the arm cart sites, *J. Appl. Meteor.*, 39, 645–665, doi:10.1175/1520-0450(2000)039<0645:ODOCHA>2.0.CO;2, 2000.
- Costantino, L., and Bréon, F. M.: Analysis of aerosol-cloud interaction from multi-sensor satellite observations. ~~Geophysical Research Letters~~Geophys. Res. Lett., 37(11), 2010.
- 10 Delle Monache, L., Perry, K.D., Cederwall, R.T. and Ogren, J.A.: In situ aerosol profiles over the Southern Great Plains cloud and radiation test bed site: 2. Effects of mixing height on aerosol properties, J. Geophys. Res., 109(D6), 2004.
- Eagan, R. C., Hobbs, P. V., and Radke, L. F.: Measurements of cloud condensation nuclei and cloud droplet size distributions in the vicinity of forest fires, ~~Journal of Applied Meteorology~~J. Appl. Meteorol., 13(5), 553-557, 1974.
- Engström, A., and Ekman, A. M.: Impact of meteorological factors on the correlation between aerosol optical depth and cloud fraction, ~~Geophysical Research Letters~~Geophys. Res. Lett., 37(18), 2010.
- 15 Feingold, G., Remer, L. A., Ramaprasad, J., and Kaufman, Y. J.: Analysis of smoke impact on clouds in Brazilian biomass burning regions: An extension of Twomey’s approach, *J. Geophys. Res.*, 106, 22907–22922, 2001.
- Feingold, G., Eberhard, W. L., Veron, D. E., and Previdi, M., “First measurements of the Twomey indirect effect using ground-based remote sensors.” ~~Geophysical Research Letters~~Geophys. Res. Lett., 30, 1287, 2003.
- 20 Feingold, G., McComiskey, A., Yamaguchi, T., Johnson J., Carslaw, K. and Schmidt, K. S.: New approaches to quantifying aerosol influence on the cloud radiative effect, *Proc. Nat. Acad. Sci.*, in press., 2016.
- Frisch, A. S., Fairall, C. W., and Snider, J. B.: Measurement of stratus cloud and drizzle parameters in ASTEX with a Ka-band Doppler radar and a microwave radiometer, ~~Journal J. of the Atmospheric Atmos. Sciences~~Sci., 52(16), 2788-2799, 1995.
- 25 Garrett, T. J., Zhao, C., Dong, X., Mace, G. G., and Hobbs, P. V.: Effects of varying aerosol regimes on low-level Arctic stratus, ~~Geophysical research letters~~Geophys. Res. Lett., 31(17), 2004.
- George, R. C., and Wood R.: Subseasonal variability of low cloud radiative properties over the southeast Pacific Ocean, ~~Atmospheric Chemistry and Physics~~Atmos. Chem. Phys. 10(8), 4047-4063, 2010.
- Ghate, V. P., Miller, M. A., Albrecht, B. A., and Fairall, C. W.: Thermodynamic and Radiative Structure of Stratocumulus-Topped Boundary Layers, *Journal of the Atmospheric Sciences*, 72(1), 430-451, 2015.
- 30 Han, Q., Rossow, W. B., Chou, J., and Welch, R. M.: Global survey of the relationships of cloud albedo and liquid water path with droplet size using ISCCP, *Journal of Climate*, 11(7), 1516-1528, 1998.

[Huang J., Q. Fu, J. Su, Q. Tang, P. Minnis, Y. Hu, Y. Yi, and Q. Zhao, 2009: Taklimakan dust aerosol radiative heating derived from CALIPSO observations using the Fu-Liou radiation model with CERES constraints, *Atmos. Chem. Phys.*, **9**, 4011-4021.](#)

5 Kaufman, Y. J., Koren, I., Remer, L. A., Rosenfeld, D., and Rudich, Y.: The effect of smoke, dust, and pollution aerosol on shallow cloud development over the Atlantic Ocean, [Proc. Nat. Acad. Sci. Proceedings of the National Academy of Sciences of the United States of America](#), 102(32), 11207-11212, 2005.

Kim, B. G., Schwartz, S. E., Miller, M. A., and Min, Q.: Effective radius of cloud droplets by ground-based remote sensing: Relationship to aerosol, [Journal of Geophysical Research: Atmospheres](#)*J. Geophys. Res.*, 108(D23), 2003.

10 Kim, B. G., Miller, M. A., Schwartz, S. E., Liu, Y., and Min, Q.: The role of adiabaticity in the aerosol first indirect effect, [Journal of Geophysical Research: Atmospheres](#)*J. Geophys. Res.* (1984–2012), 113(D5), 2008.

Klein, S. A., and Hartmann, D. L.: The seasonal cycle of low stratiform clouds, *Journal of Climate*, 6.8, 1587-1606, 1993.

Koren, I., Martins, J. V., Remer, L. A., Afargan, H.: Smoke invigoration versus inhibition of clouds over the Amazon, *Science*, 321, 946, 2008.

15 Koren, I., Altaratz, O., Remer, L. A., Feingold, G., Martins, J. V., and Heiblum, R. H.: Aerosol-induced intensification of rain from the tropics to the mid-latitudes, *Nature Geoscience*, 5(2), 118-122, 2012.

Liu, Y., W. Wu, M. P. Jensen, and T. Toto: Relationship between cloud radiative forcing, cloud fraction and cloud albedo, and new surface-based approach for determining cloud albedo, *Atmos. Chem. Phys*, 11, 7155-7170, doi:10.5194/acp-11-7155-2011, 2011.

20 Long, C. N., and Ackerman, T. P.: Identification of clear skies from broadband pyranometer measurements and calculation of downwelling shortwave cloud effects, [Journal of Geophysical Research: Atmospheres](#)*J. Geophys. Res.*, 105(D12), 15609-15626, 2000.

Long, C. N., and Shi, Y.: The QCRad value added product: Surface radiation measurement quality control testing, including climatology configurable limits, Atmospheric Radiation Measurement Program Technical Report, 2006.

25 Long, C. N., Ackerman, T. P., Gaustad, K. L., and Cole, J. N. S.: Estimation of fractional sky cover from broadband shortwave radiometer measurements, [Journal of Geophysical Research: Atmospheres](#)*J. Geophys. Res.*, 111(D11), 2006.

McComiskey, A, Feingold, G., Frisch, A. S., Turner, D. D., Miller, M., Chiu, J. C., Min, Q., and Ogren, J.: An assessment of aerosol-cloud interactions in marine stratus clouds based on surface remote sensing, *J. Geophys. Res.*, 114, D09203, 2009.

McComiskey A. and Feingold, G.: The scale problem in quantifying aerosol indirect effects, [Atmospheric Chemistry and Physics](#)*Atmos. Chem. Phys.*, 12, 1031–1049, 2012.

30 Min, Q. and Harrison, L. C.: Cloud properties derived from surface MFRSR measurements and comparison with GOES results at the ARM SGP site, [Geophysical Research Letters](#)*Geophys. Res. Lett.*, 23, 1641-1644, 1996.

Nakajima, T., Higurashi, A., Kawamoto, K., and Penner, J. E.: A possible correlation between satellite-derived cloud and aerosol microphysical parameters, [Geophysical Research Letters](#)*Geophys. Res. Lett.*, 28(7), 1171-1174, 2001.

Platnick, S., and Twomey, S.: Determining the susceptibility of cloud albedo to changes in droplet concentration with the

- Advanced Very High Resolution Radiometer, ~~Journal of Applied Meteorology~~[J. Appl. Meteorol.](#), 33(3), 334-347, 1994.
- Quaas, J., Boucher, O., Bellouin, N., and Kinne, S.: Satellite-based estimate of the direct and indirect aerosol climate forcing, ~~Journal of Geophysical Research: Atmospheres~~[J. Geophys. Res.](#) (1984–2012), 113(D5), 2008.
- Sheridan, P. J., Delene, D. J., and Ogren, J. A.: Four years of continuous surface aerosol measurements from the Department of Energy's Atmospheric Radiation Measurement Program Southern Great Plains Cloud and Radiation Testbed site, ~~Journal of Geophysical Research~~[J. Geophys. Res.](#), 106 (D18), 20735-20747, 2001.
- Small, J. D., Chuang, P. Y., Feingold, G., and Jiang, H.: Can aerosol decrease cloud lifetime?, ~~Geophysical Research Letters~~[Geophys. Res. Lett.](#), 36(16), 2009.
- Stephens, G. L., Paltridge, G. W., and Platt, C. M. R.: Radiation profiles in extended water clouds - III: Observations, ~~Journal of the Atmospheric Sciences~~[Sci.](#), 35(11), 2133-2141, 1978
- Stevens, B., and Feingold, G.: Untangling aerosol effects on clouds and precipitation in a buffered system, *Nature*, 461(7264), 607-613, 2009.
- Trenberth, K. E., Fasullo, J. T., and Kiehl, J.: Earth's global energy budget, ~~Bull. Amer. Meteor. Soc.~~[Bulletin of the American Meteorological Society](#), 90(3), 311-323, 2009.
- 15 Troyan, D.: Merged Sounding Value-Added Product Technical Report. U.S, Department of Energy, DOE/SC-ARM-TR-087, 2012.
- Turner, D. and Min, Q.: Cloud Optical Properties from the Multi-Filter Shadowband Radiometer (MFRSRCLDOD): An ARM Value-Added Product Technical Report. U.S, Department of Energy, DOE/SC-ARM-TR-047, 2004.
- Turner, D.D., Clough, S. A., Liljegren, J. C., Clothiaux, E. E., Cady-Pereira, K., and Gaustad, K. L.: Retrieving liquid water path and precipitable water vapor from Atmospheric Radiation Measurement (ARM) microwave radiometers, *IEEE Trans. Geosci. Remote Sens.*, 45, 3680-3690, doi:10.1109/TGRS.2007.903703, 2007a.
- Turner, D. D., Vogelmann, A. M., Austin, R. T., Barnard, J. C., Cady-Pereira, K., Chiu, J. C., Clough, S. A., Flynn, C., Khaiyer, M.M., Liljegren, J. and Johnson, K.: Thin liquid water clouds: Their importance and our challenge, ~~Bull. Amer. Meteor. Soc.~~[Bulletin of the American Meteorological Society](#), 88(2), 177-190, 2007b.
- 25 Twohy, C. H., Petters, M. D., Snider, J. R., Stevens, B., Tahnk, W., Wetzel, M., Russell, L. and Burnet, F.: Evaluation of the aerosol indirect effect in marine stratocumulus clouds: Droplet number, size, liquid water path, and radiative impact, ~~Journal of Geophysical Research: Atmospheres~~[J. Geophys. Res.](#), 110(D8), 2005
- Twomey, S.: The nuclei of natural cloud formation part II: The supersaturation in natural clouds and the variation of cloud droplet concentration, *Geofisica pura e applicata*, 43(1), 243-249, 1959.
- 30 Twomey, S.: Pollution and the planetary albedo, *Atmos. Environ.*, 8, 1251–1256, 1974.
- Twomey, S.: The influence of pollution on the shortwave albedo of clouds, *J. Atmos. Sci.*, 34, 1149 – 1152, 1977.
- Vavrus, S.: An alternative method to calculate cloud radiative forcing: Implications for quantifying cloud feedbacks, ~~Geophysical research letters~~[Geophys. Res. Lett.](#), 33(1), 2006.
- Vogelmann, A. M., McFarquhar, G. M., Ogren, J. A., Turner, D. D., Comstock, J. M., Feingold, G., Long, C. N., Jonsson, H.

H., Bucholtz, A., Collins, D. R. and Diskin, G. S.: RACORO extended-term aircraft observations of boundary layer clouds, [Bull. Amer. Meteor. Soc.](#), ~~Bulletin of the American Meteorological Society~~ 93(6), 861-878, 2012.

Warner, J., and Twomey, S.: The production of cloud nuclei by cane fires and the effect on cloud droplet concentration, [Journal of the atmospheric sciences](#), 24(6), 704-706, 1967.

5 Wen, G., Marshak, A., Cahalan, R.F., Remer, L.A. and Kleidman, R.G.: 3-D aerosol-cloud radiative interaction observed in collocated MODIS and ASTER images of cumulus cloud fields, [Journal of Geophysical Research: Atmospheres](#), 112(D13), 2007.

Wood, R., and Bretherton, C. S.: On the relationship between stratiform low cloud cover and lower-tropospheric stability, *Journal of climate*, 19(24), 6425-6432, 2006.

10 Xie, Y., and Liu, Y.: A new approach for simultaneously retrieving cloud albedo and cloud fraction from surface-based shortwave radiation measurements, *Environmental Research Letters*, 8(4), 044023, 2013.

15

20

25

30

Table 1: List of the measurements, retrievals and ARM instruments at the Southern Great Plains used in this study.

<i>Instrument</i>	<i>Resolution in the original data set</i>	<i>Measurement / Retrieval</i>
Milimeter Wavelength Cloud Radar (MMCR)	10 s	Column Maximum Reflectivity (Z_{max})
Ceilometer / Micropulse Lidar (MPL)	10 s	Cloud base height (h_{CB})
MMCR / MPL	10 s	Cloud top height (h_{CT})
MMCR + Ceilometer	10 s	Doppler vertical velocity at h_{CB} (w)
Microwave Radiometer (MWR)	20 s	Liquid water path (LWP)
		Relative cloud radiative effect (rCRE)
Broadband radiometers	1 min	Cloud optical depth (τ_c) Cloud fraction (f_c) Cloud albedo (A_c)
Nephelometer	1 min	Scattering at 550 nm (σ_{550nm}) Ångström exponent (Å)
Meteorological station (MET)	1 min	Lifting condensation level (LCL)
Radiosondes + MET + MWR + Models	1 min	Lower tropospheric stability (LTS)

5

10

15

Table 2: Slopes α and their uncertainty obtained using different τ_c retrievals: from the Radiative Flux Analysis (RFA) , using the Xie and Liu technique (2013, XL) and using MFRSR measurements. Coincident retrievals of τ_c from each retrieval acquired when $\theta_0 < 70^\circ$, for each day were used to calculate α .

	$LWP (g m^{-2})$	α_{RFA}	α_{XL}	α_{MFRSR}
<i>Case study 1</i>	50 - 75	0.27 ± 0.09	0.32 ± 0.09	0.23 ± 0.07
	75 - 100	0.26 ± 0.07	-0.03 ± 0.08	0.25 ± 0.06
	100 - 150	0.73 ± 0.26	0.58 ± 0.30	0.70 ± 0.24
<i>Case study 2</i>	50 - 75	-0.01 ± 0.09	0.31 ± 0.07	0.10 ± 0.06
	75 - 100	-0.09 ± 0.04	0.25 ± 0.04	0.07 ± 0.03
	100 - 150	-0.23 ± 0.04	0.11 ± 0.02	-0.03 ± 0.02

10

15

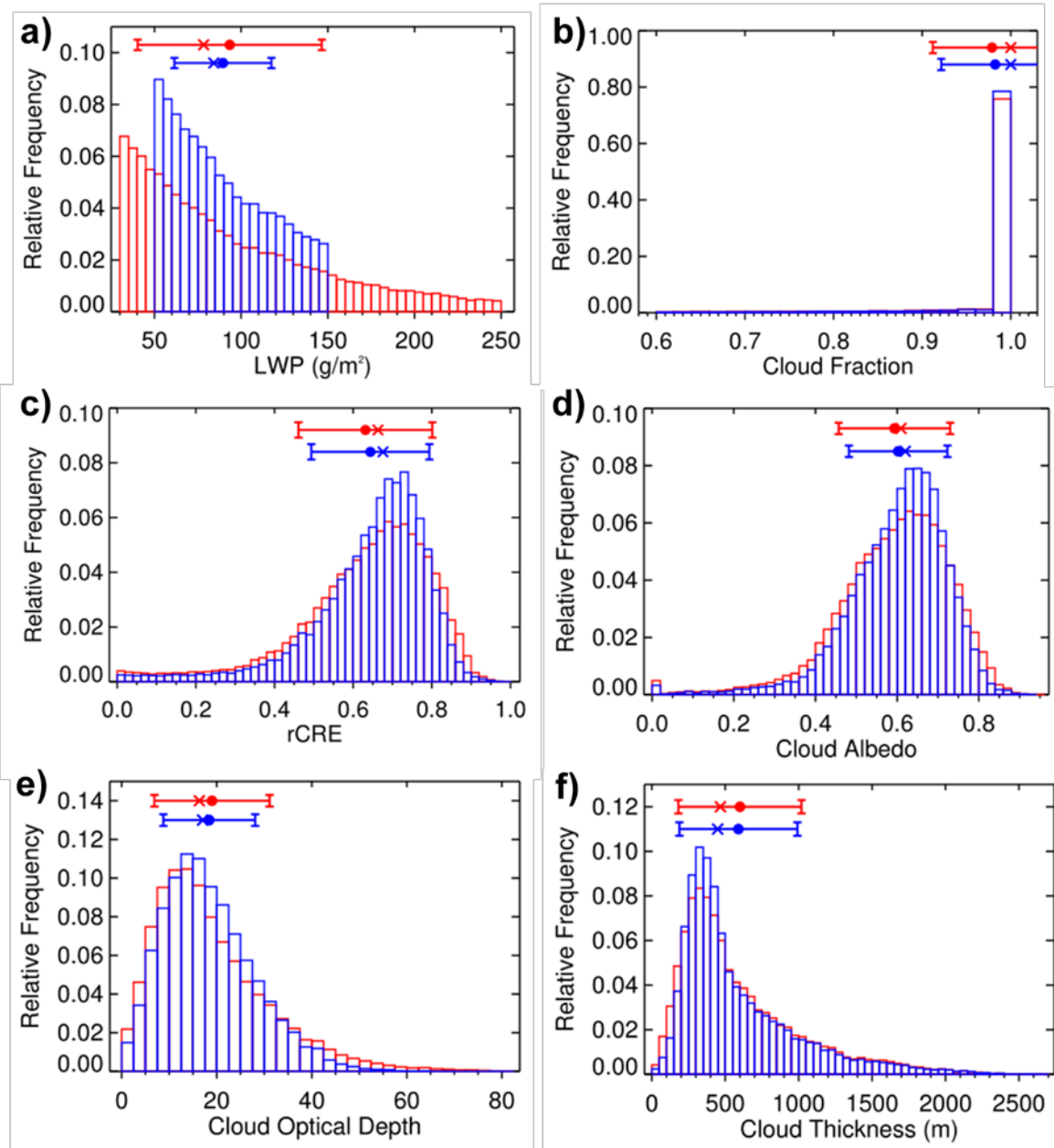


Figure 1: Statistical distributions of: a) liquid water path (LWP), b) cloud fraction (f_c), c) rCRE, d) cloud albedo (A_c), e) cloud optical depth (τ_c), f) cloud thickness, g) cloud base height (h_{CB}), h) cloud top height (h_{CT}), i) aerosol index (A_i), j) $w'^2 = [w-w_0]^2$, k) decoupling index (D_i), l) lower tropospheric stability (LTS).

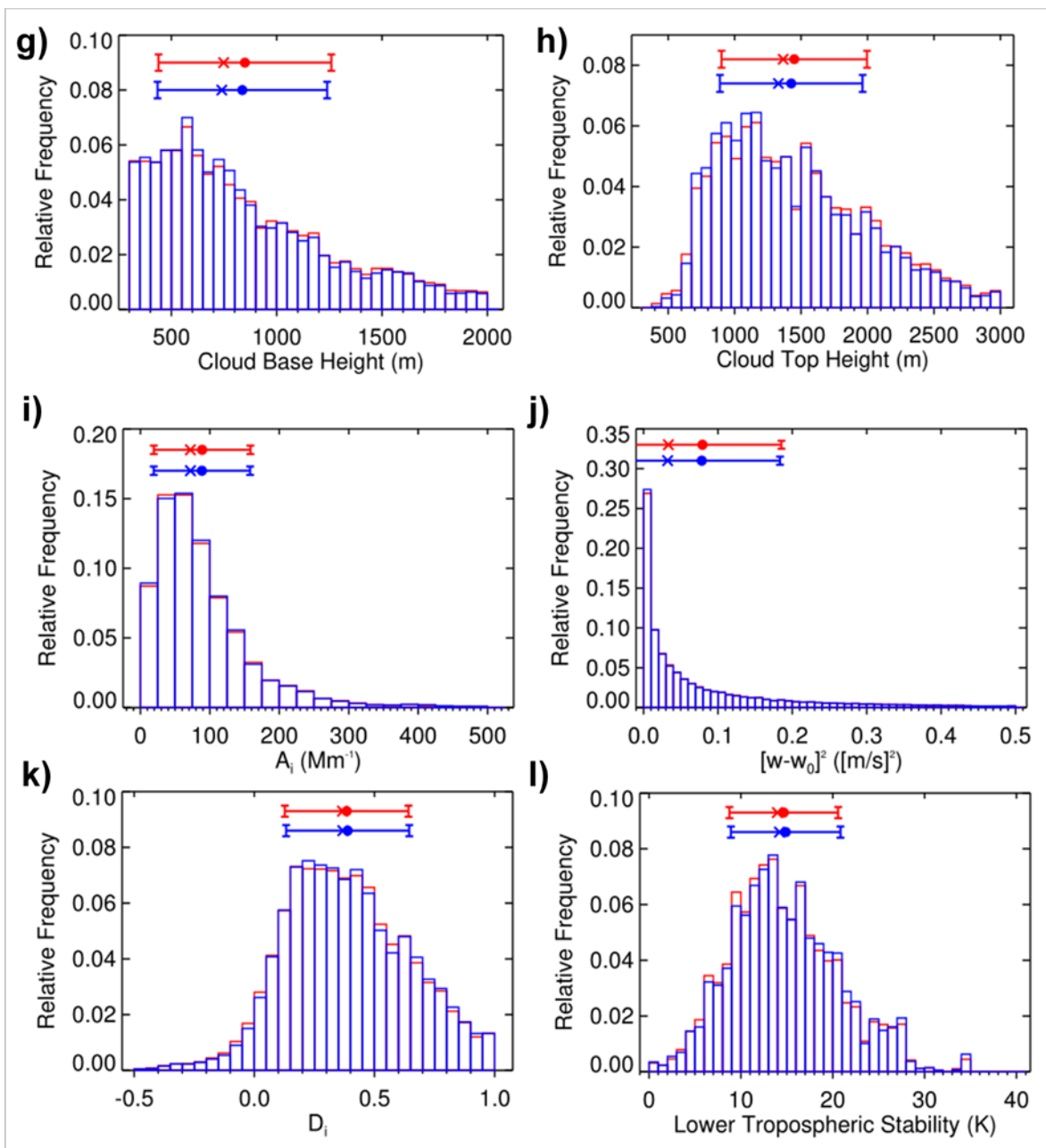


Figure 1: continued.

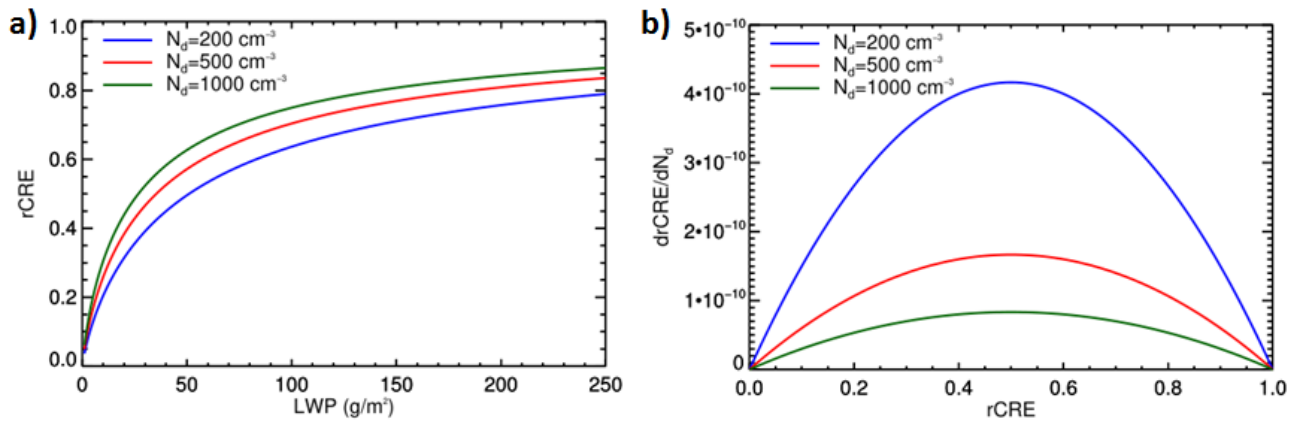


Figure 2: Theoretical approximations of a) rCRE as a function of LWP, and b) cloud radiative susceptibility to N_d as a function of rCRE for different droplet concentrations: $N_d = 200 \text{ cm}^{-3}$ (blue), $N_d = 500 \text{ cm}^{-3}$ (red) and $N_d = 1000 \text{ cm}^{-3}$ (green).

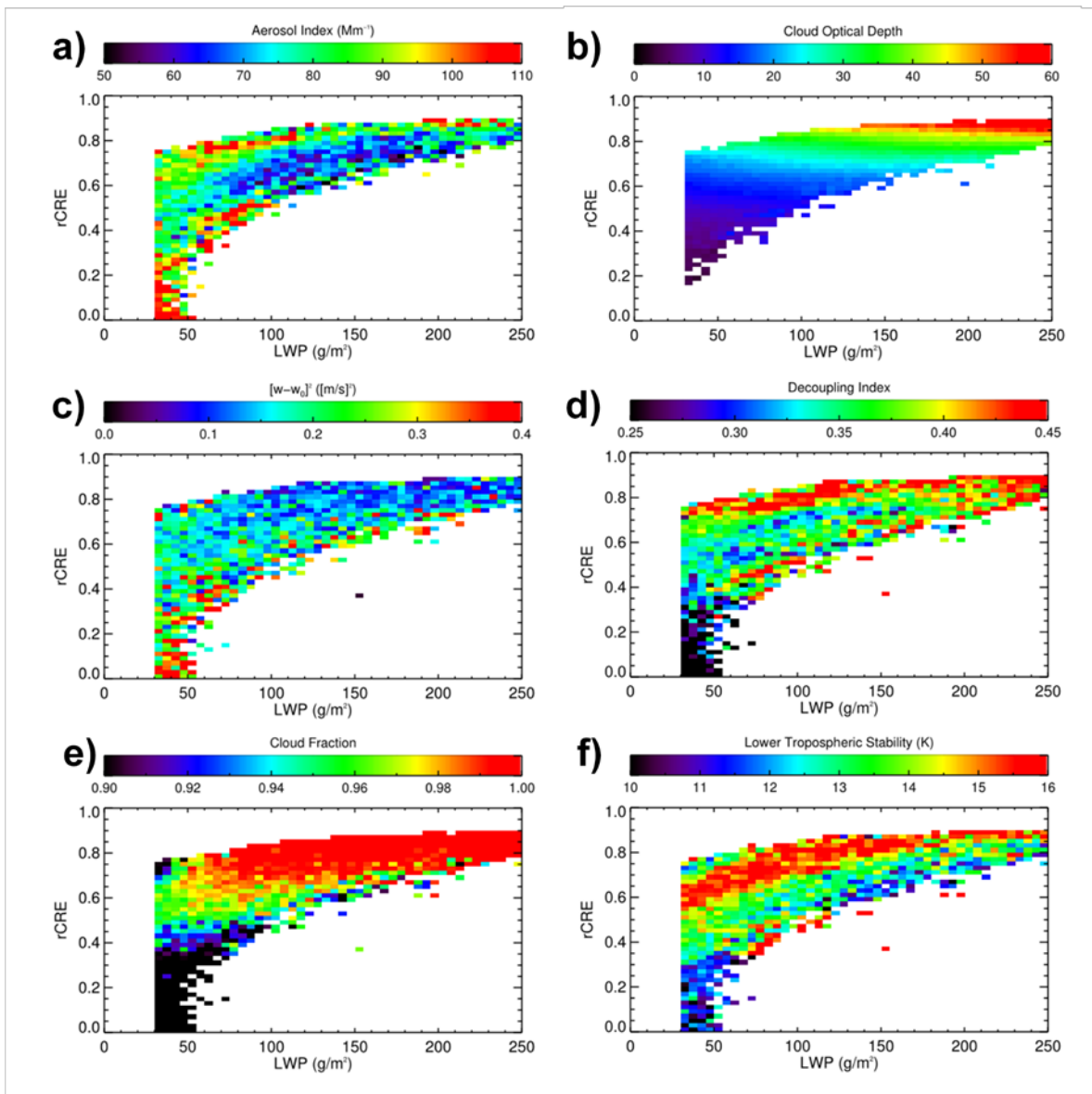


Figure 3: Relative cloud radiative effect as a function of liquid water path colored by a) aerosol index, b) cloud optical depth, c) w^2 , d) decoupling index, e) cloud fraction and f) lower tropospheric stability.

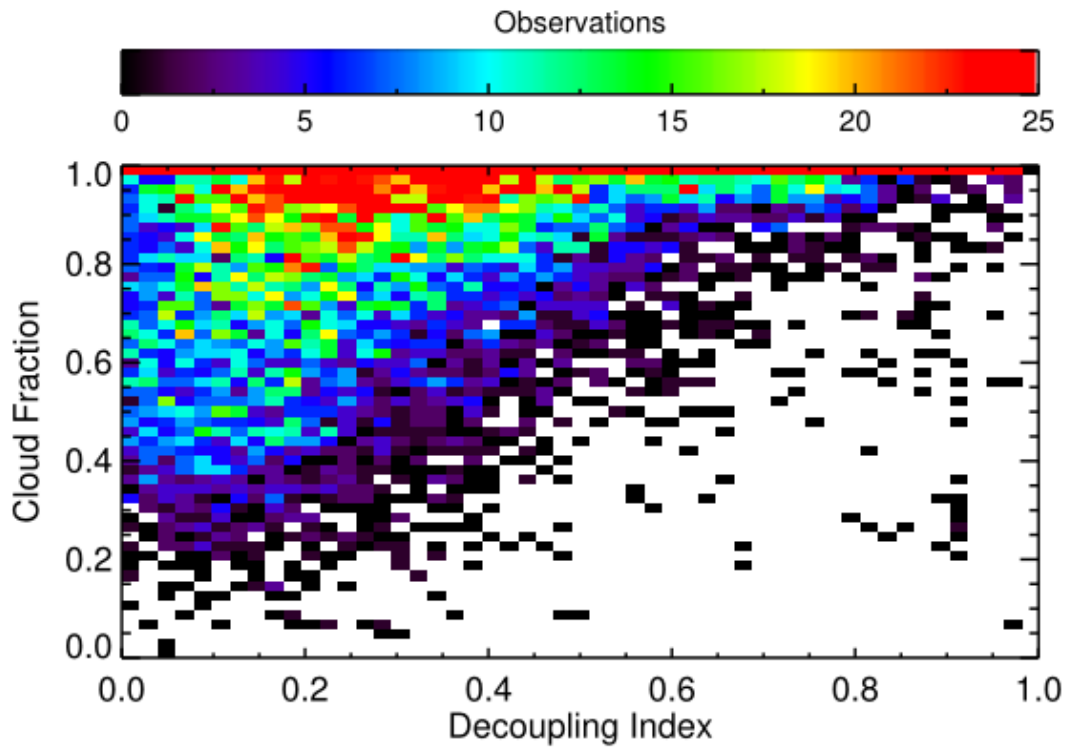


Figure 4: Joint probability distribution function of D_i and f_c obtained from 14-years of observations at SGP.

5
10
15

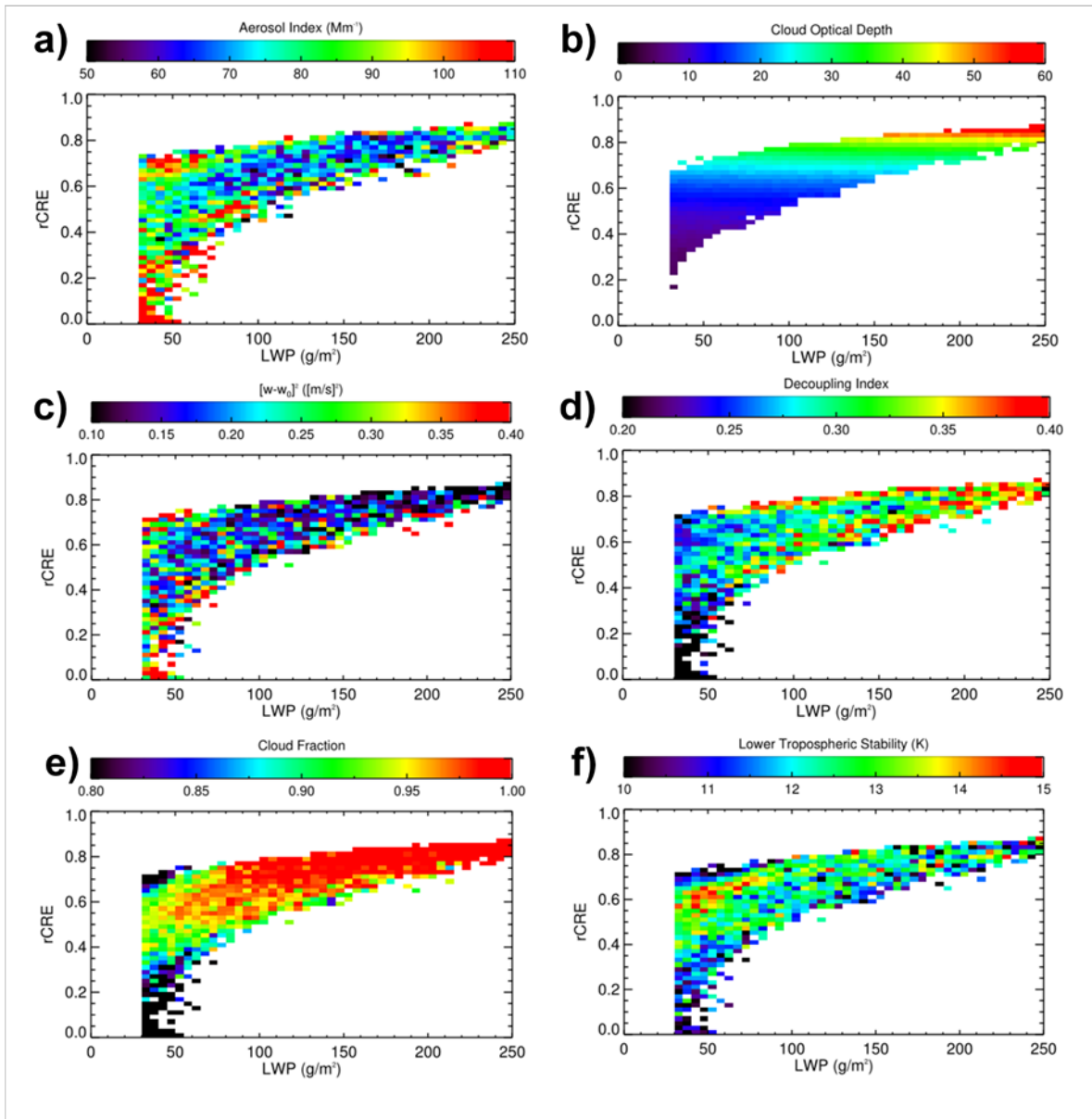


Figure 5: Relative cloud radiative effect as a function of liquid water path colored by a) aerosol index, b) cloud optical depth, c) w^2 , d) decoupling index, e) cloud fraction and f) lower tropospheric stability for $\cos(\theta_0) \geq 0.6$.

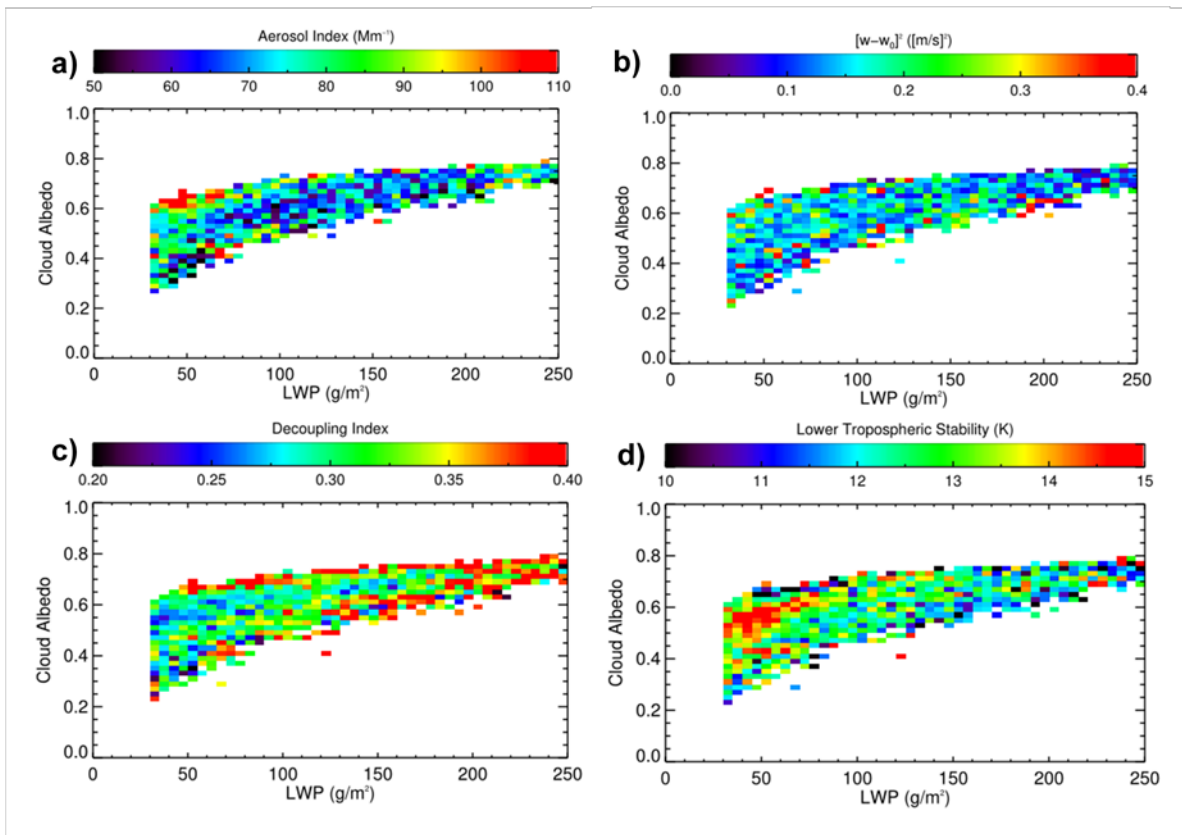


Figure 6S: Cloud albedo as a function of liquid water path colored by a) aerosol index, b) w'^2 , c) decoupling index and d) lower tropospheric stability, for completely overcast conditions ($f_c = 1$) for $\cos(\theta_0) \geq 0.6$.

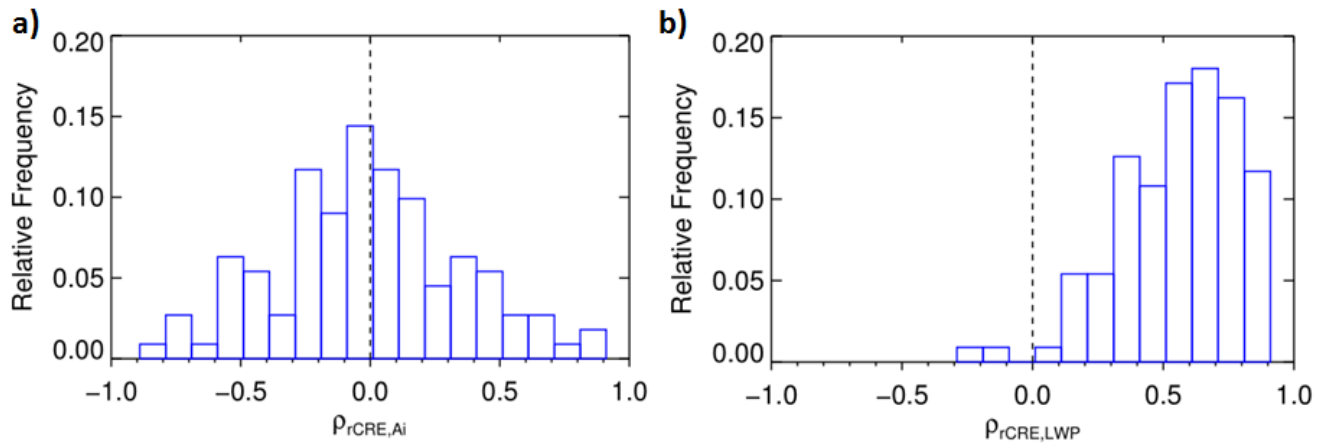


Figure 76: Daily distribution of the a) correlation between the relative cloud radiative effect (rCRE) and aerosol index (A_i) and b) the correlation between rCRE and liquid water path (LWP) for $\cos(\theta_0) \geq 0.6$.

5

10

15

20

25

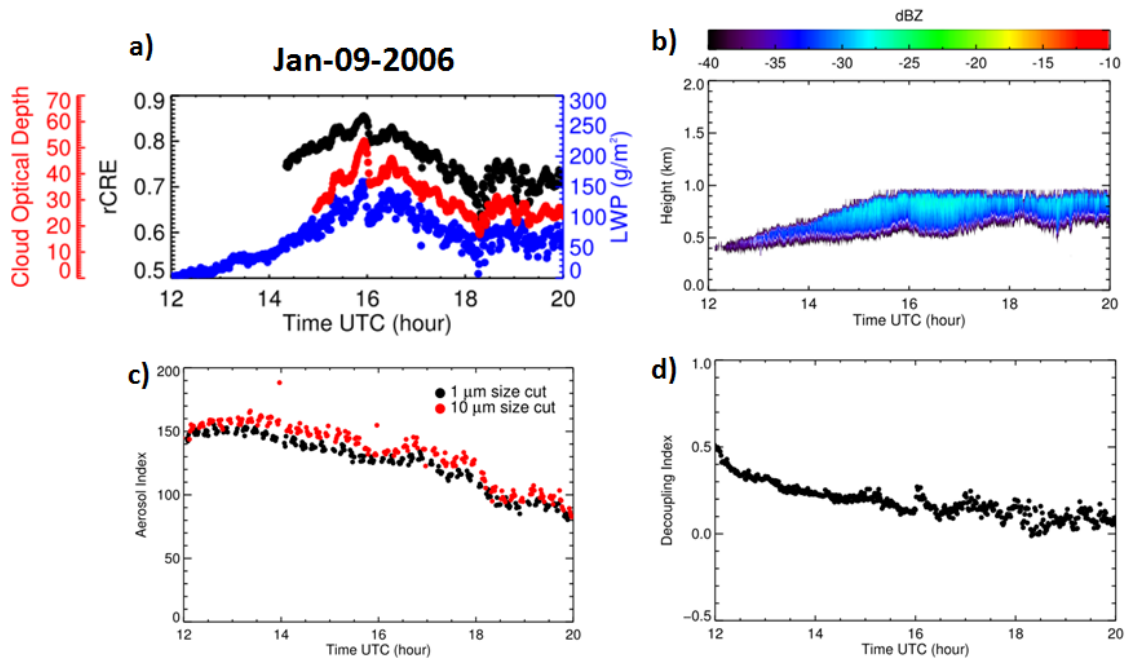


Figure 8: Time series of: a) rCRE, cloud optical depth and LWP, b) vertical profile of radar reflectivity, c) aerosol index, and d) decoupling index for January 9th 2006.

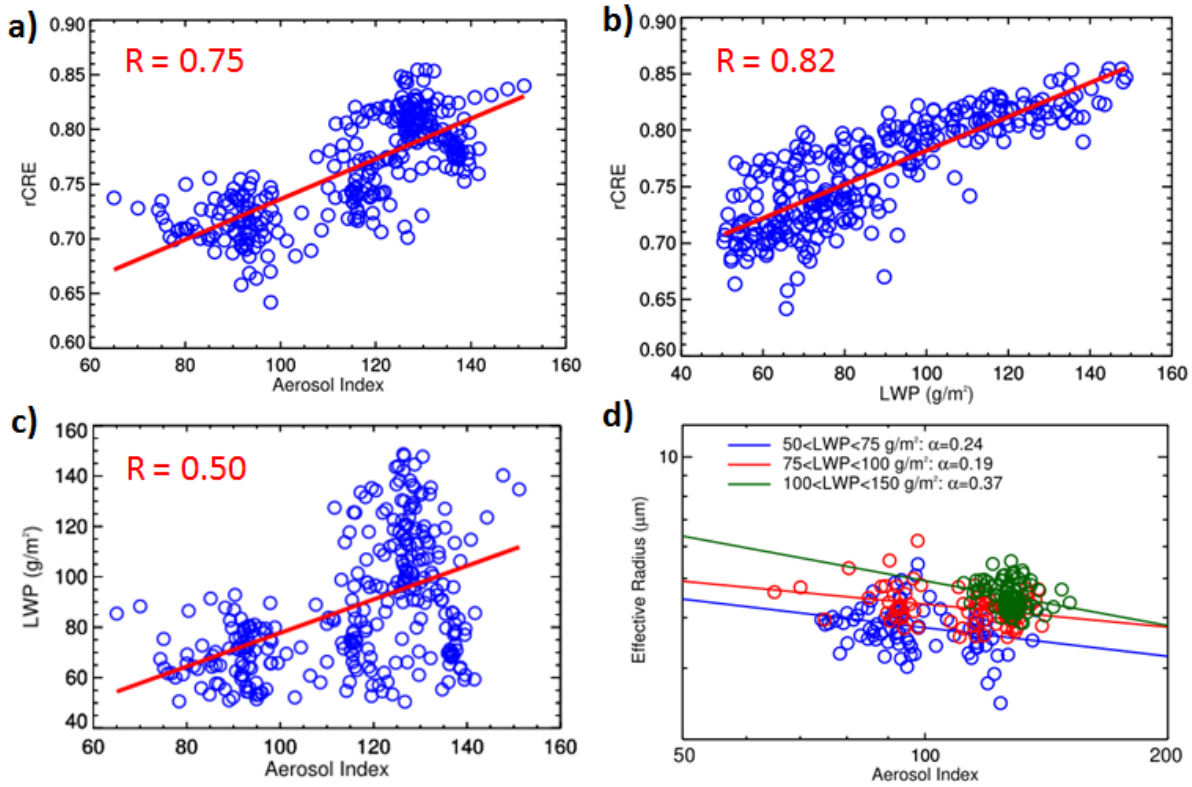


Figure 9: Correlation between a) rCRE and A_i , b) rCRE and LWP, c) LWP and A_i and d) effective radius as a function of A_i grouped by LWP for January 9th 2006.

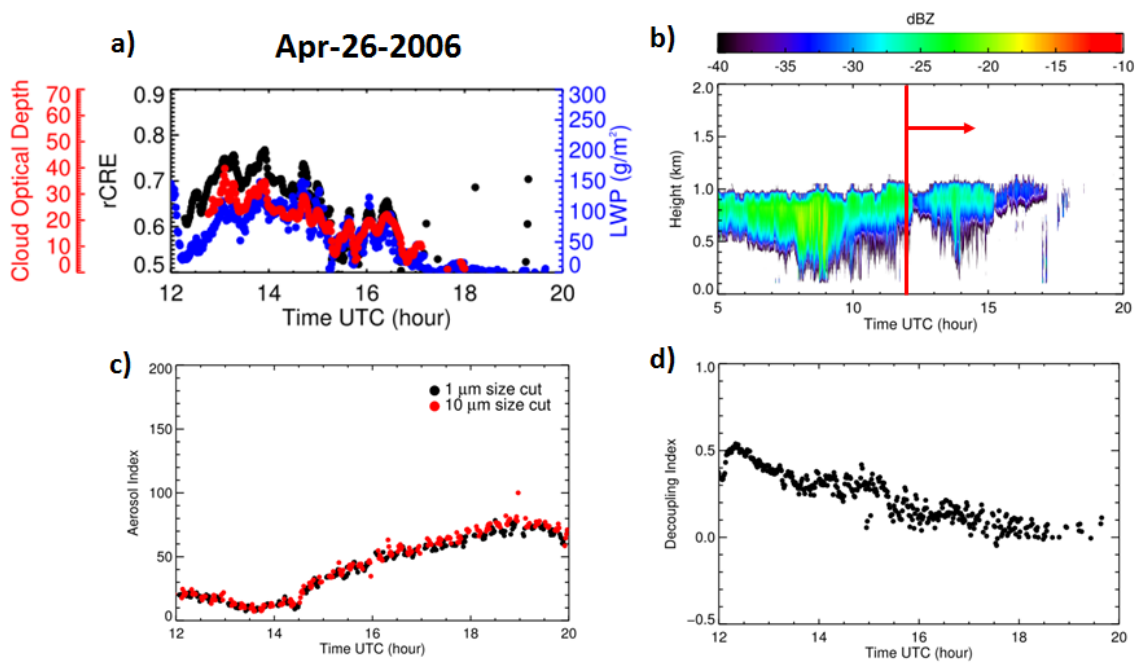


Figure 10: Time series of: a) rCRE, cloud optical depth and LWP, b) radar reflectivity, c) aerosol index, and d) decoupling index for April 26th 2006.

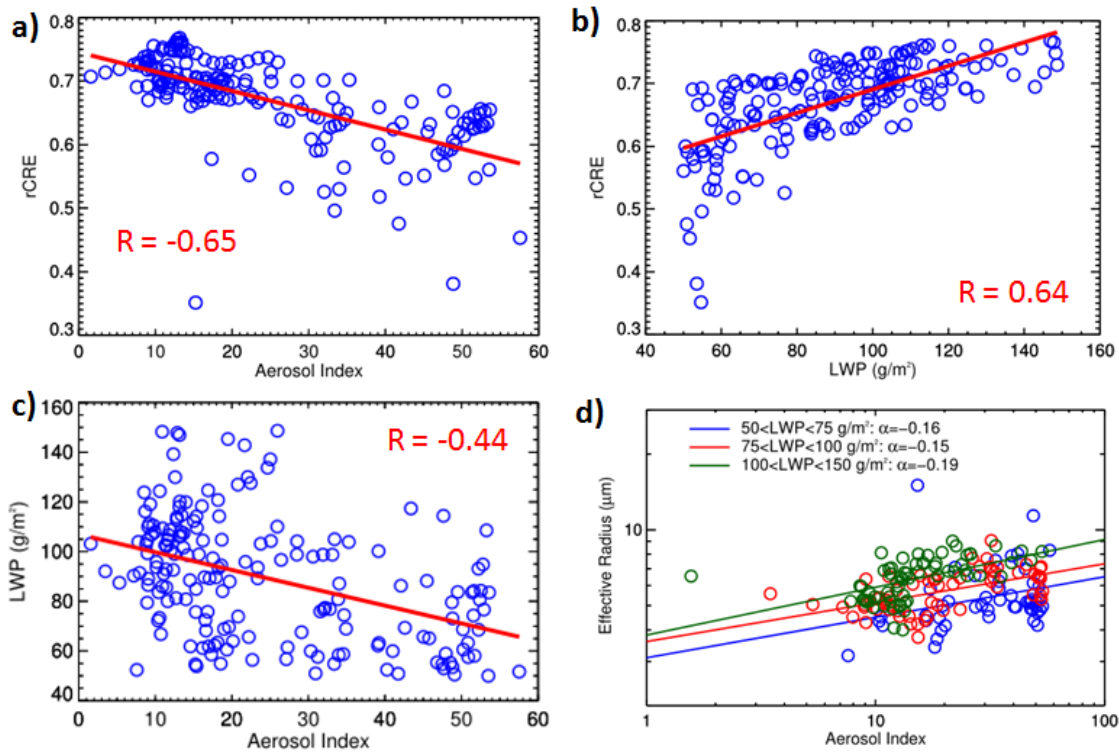


Figure 11: Correlation between a) rCRE and A_i , b) rCRE and LWP, c) LWP and A_i and d) effective radius as a function of A_i grouped by LWP for April 26th 2006.

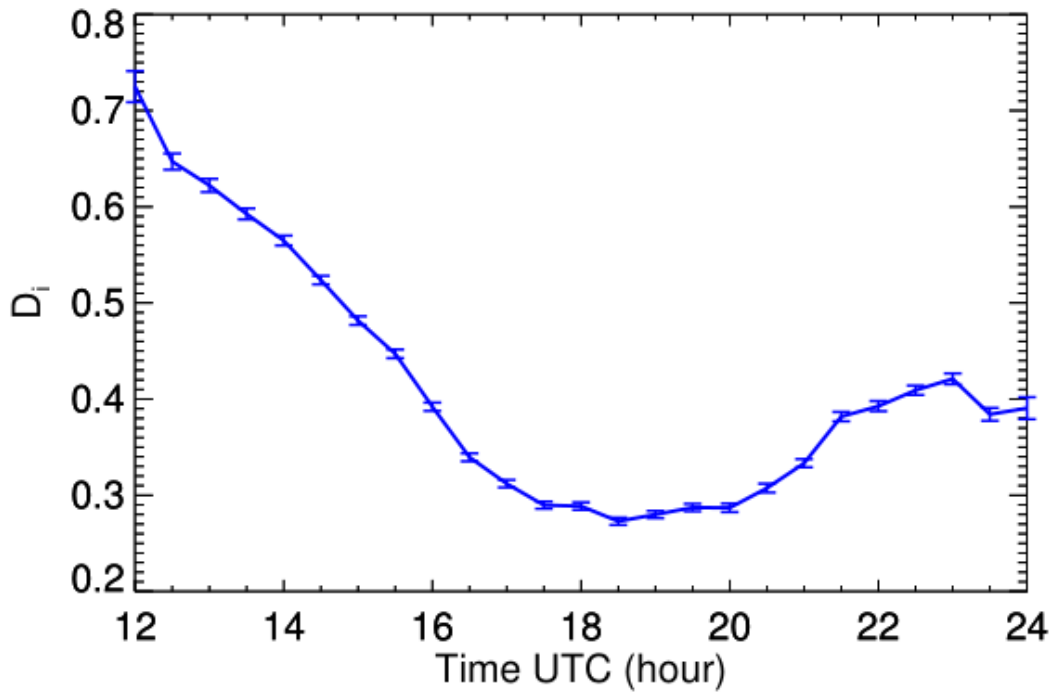


Figure 12: Mean diurnal cycle of the decoupling index (D_i) obtained using 14 years of retrievals at the SGP. Error bars indicate the standard deviation of the mean for each time bin.

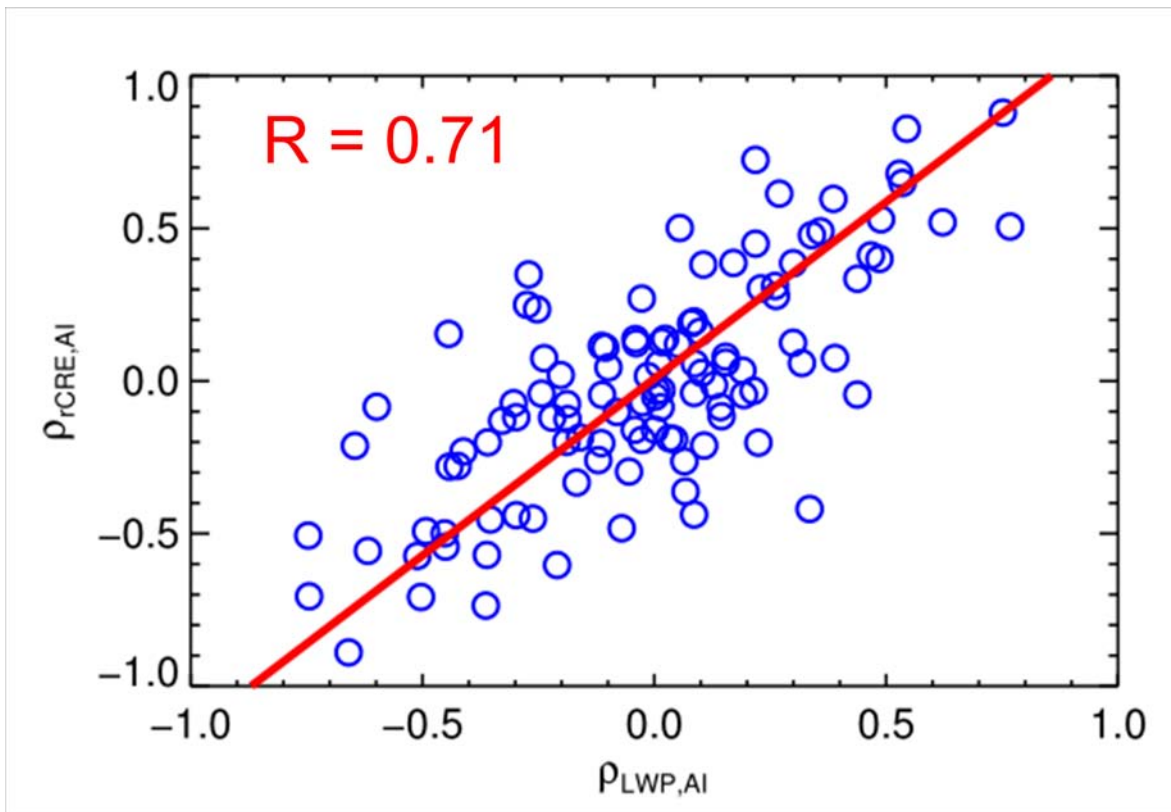


Figure 13: Correlation between rCRE and A_i ($\rho_{rCRE,Ai}$) versus the correlation between LWP and A_i ($\rho_{LWP,Ai}$) for $\cos(\theta_0) \geq 0.6$.